The Two-Surface Wave Decay process in ultrashort, high intensity laser-plasma interactions

Andrea Macchi

Istituto Nazionale per la Fisica della Materia (INFM)

Dipartimento di Fisica "Enrico Fermi", Università di Pisa

`www.df.unipi.it/∼macchi`

CELIA, Université Bordeaux I, January 22th 2004

Contributors

Fulvio Cornolti, Francesco Pegoraro (supervision)

Contributors

Fulvio Cornolti, Francesco Pegoraro (supervision)

Marco Battaglini (analytical work)

Contributors

Fulvio Cornolti, Francesco Pegoraro (supervision)

Marco Battaglini (analytical work)

Federica Cattani (test particle simulations)

Contributors

Fulvio Cornolti, Francesco Pegoraro (supervision)

Marco Battaglini (analytical work)

Federica Cattani (test particle simulations)

Tatiana V. Liseikina (PIC simulations)

Contributors

Fulvio Cornolti, Francesco Pegoraro (supervision)

Marco Battaglini (analytical work)

Federica Cattani (test particle simulations)

Tatiana V. Liseikina (PIC simulations)

Hartmut Ruhl[1], Vitaly A. Vshivkov[2] (early code development)

---

[1]University of Reno, Nevada, US

[2]Institute for Computational Technologies, Novosibirsk, Russia

Outlook

- The interaction regime

Outlook

- The interaction regime
- The two-surface wave decay idea

Outlook

- The interaction regime
- The two-surface wave decay idea
  - Numerical observations

Outlook

- The interaction regime
- The two-surface wave decay idea
  - Numerical observations
  - Analytical theory

Outlook

- The interaction regime
- The two-surface wave decay idea
  - Numerical observations
  - Analytical theory
- TSWD effects on fast electron generation

Outlook

- The interaction regime
- The two-surface wave decay idea
  - Numerical observations
  - Analytical theory
- TSWD effects on fast electron generation
- Future directions

Interaction regime

- Laser pulse: **high intensity** ($I_L \sim 10^{18}$ W/cm^2), **short duration** ($\tau_L \leq 100$ fs)

Interaction regime

- Laser pulse: **high intensity** ($I_L \sim 10^{18}$ W/cm^2), **short duration** ($\tau_L \leq 100$ fs)

- Plasma: **overdense** ($n_e \geq n_c \sim 10^{21}$ cm^{-3}), **step boundary** ($L = n_c / |\boldsymbol{\nabla} n_e|_{@n_c} \ll \lambda_L$)

Interaction regime

- Laser pulse: **high intensity** ($I_L \sim 10^{18}$ W/cm^2), **short duration** ($\tau_L \leq 100$ fs)

- Plasma: **overdense** ($n_e \geq n_c \sim 10^{21}$ cm^{-3}), **step boundary** ($L = n_c/|\boldsymbol{\nabla} n_e|_{@n_c} \ll \lambda_L$)

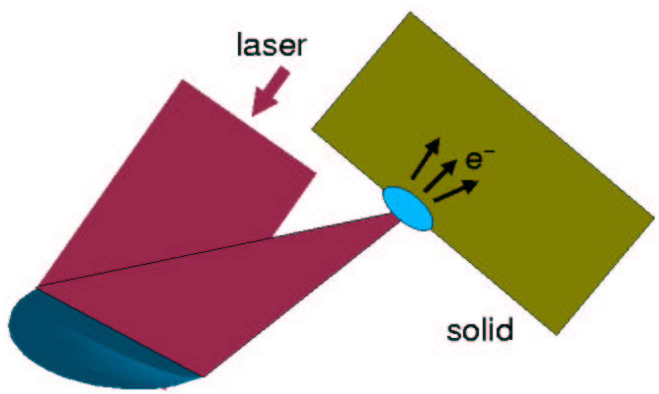

Interaction regime

- Laser pulse: **high intensity** ($I_L \sim 10^{18}$ W/cm^2), **short duration** ($\tau_L \leq 100$ fs)
- Plasma: **overdense** ($n_e \geq n_c \sim 10^{21}$ cm^{-3}), **step boundary** ($L = n_c/|\boldsymbol{\nabla} n_e|_{@n_c} \ll \lambda_L$)

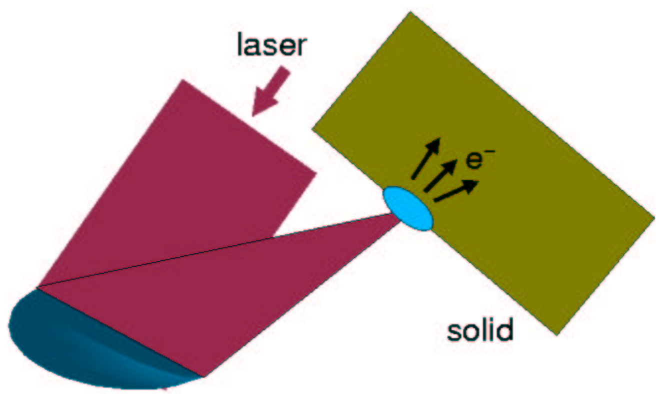

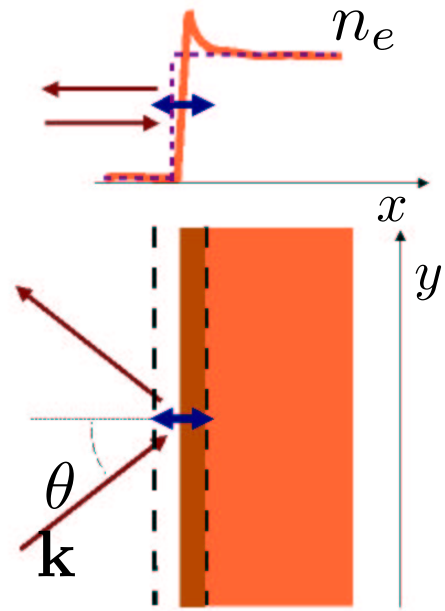

Interaction regime

- Laser pulse: **high intensity** ($I_L \sim 10^{18}$ W/cm^2), **short duration** ($\tau_L \leq 100$ fs)

- Plasma: **overdense** ($n_e \geq n_c \sim 10^{21}$ cm^{-3}), **step boundary** ($L = n_c/|\boldsymbol{\nabla} n_e|_{@n_c} \ll \lambda_L$)

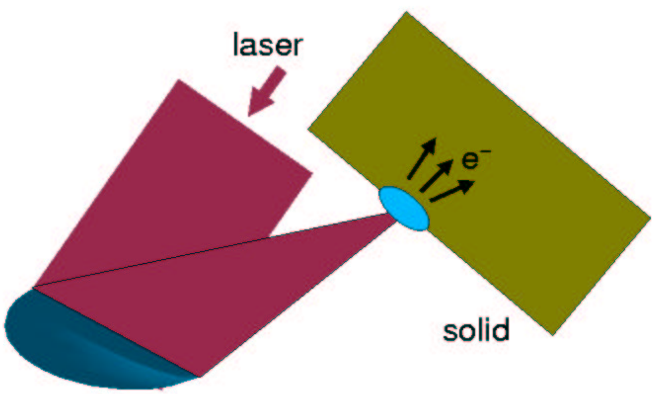

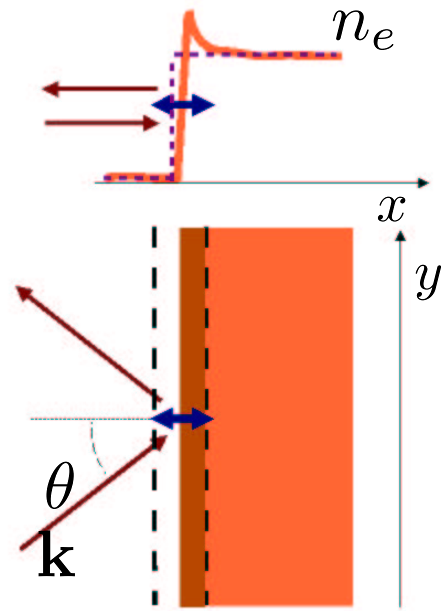

Force driving the plasma surface: $\mathbf{F} = -e(\underbrace{\mathbf{E}}_{\omega} + \underbrace{\mathbf{v} \times \mathbf{B}}_{2\omega})$

Interaction regime

- Laser pulse: **high intensity** ($I_L \sim 10^{18}$ W/cm^2), **short duration** ($\tau_L \leq 100$ fs)

- Plasma: **overdense** ($n_e \geq n_c \sim 10^{21}$ cm^{-3}), **step boundary** ($L = n_c/|\boldsymbol{\nabla} n_e|_{@n_c} \ll \lambda_L$)

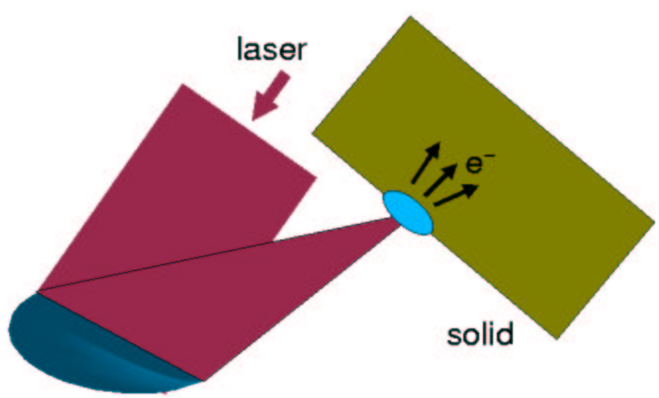

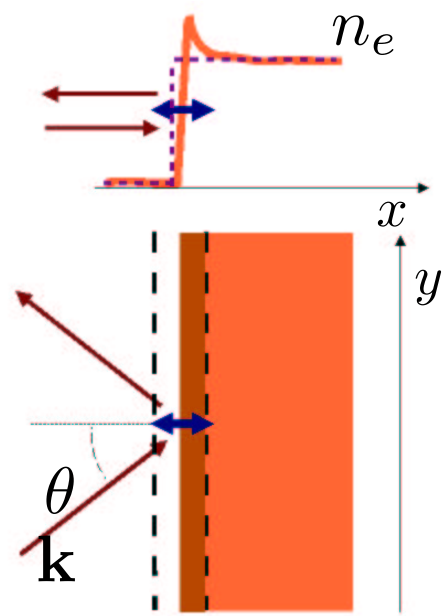

Force driving the plasma surface: $\mathbf{F} = -e(\underbrace{\mathbf{E}}_{\omega} + \underbrace{\mathbf{v} \times \mathbf{B}}_{2\omega})$

(strong dependence on polarization and incidence angle)

Routes to collisionless absorption

Dominance of collisionless absorption at high irradiances $\geq 10^{16}$ W/cm^2 is well established experimentally.

Routes to collisionless absorption

Dominance of collisionless absorption at high irradiances $\geq 10^{16}$ W/cm^2 is well established experimentally.

Two "classes" of collisionless absorption mechanisms:

Routes to collisionless absorption

Dominance of collisionless absorption at high irradiances $\geq 10^{16}$ W/cm^2 is well established experimentally.

Two "classes" of collisionless absorption mechanisms:

- kinetic effects

Routes to collisionless absorption

Dominance of collisionless absorption at high irradiances $\geq 10^{16}$ W/cm^2 is well established experimentally.

Two "classes" of collisionless absorption mechanisms:

- kinetic effects,e.g.
  - anomalous skin effect

Routes to collisionless absorption

Dominance of collisionless absorption at high irradiances $\geq 10^{16}$ W/cm^2 is well established experimentally.

Two "classes" of collisionless absorption mechanisms:

- kinetic effects,e.g.
  - anomalous skin effect
  - interface phase mixing or "vacuum heating"
- mode conversion

Routes to collisionless absorption

Dominance of collisionless absorption at high irradiances $\geq 10^{16}$ W/cm^2 is well established experimentally.

Two "classes" of collisionless absorption mechanisms:

- kinetic effects,e.g.
  - anomalous skin effect
  - interface phase mixing or "vacuum heating"
- mode conversion, e.g. excitation of

Routes to collisionless absorption

Dominance of collisionless absorption at high irradiances $\geq 10^{16}$ W/cm^2 is well established experimentally.

Two "classes" of collisionless absorption mechanisms:

- kinetic effects,e.g.
  - anomalous skin effect
  - interface phase mixing or "vacuum heating"
- mode conversion, e.g. excitation of
  - plasma waves (resonance absorption)

Routes to collisionless absorption

Dominance of collisionless absorption at high irradiances $\geq 10^{16}$ W/cm^2 is well established experimentally.

Two "classes" of collisionless absorption mechanisms:

- kinetic effects,e.g.
  - anomalous skin effect
  - interface phase mixing or "vacuum heating"

- mode conversion, e.g. excitation of
  - plasma waves (resonance absorption)
  - **surface waves**

Electron surface waves (cold plasma)

Step boundary, overdense plasma:

$n_i = n_0\theta(x)$, $n_0 > 2n_c$

Electron surface waves (cold plasma)

Step boundary, overdense plasma:

$n_i = n_0\theta(x)$, $n_0 > 2n_c$

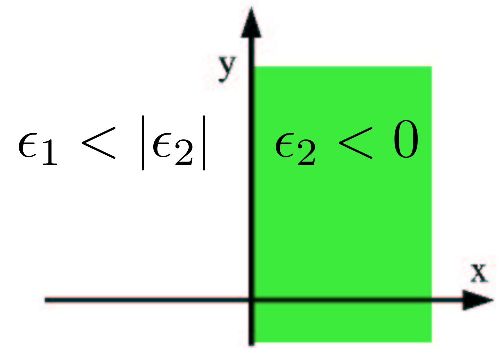

$$\epsilon_2 = 1 - \frac{\omega_p^2}{\omega^2} = 1 - \frac{n_e}{n_c} < -1$$

Electron surface waves (cold plasma)

Step boundary, overdense plasma:

$n_i = n_0\theta(x)$, $n_0 > 2n_c$

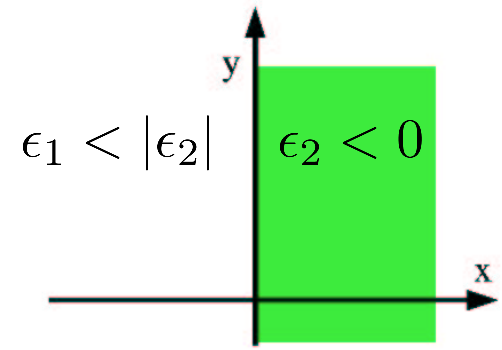

$$\epsilon_2 = 1 - \frac{\omega_p^2}{\omega^2} = 1 - \frac{n_e}{n_c} < -1$$

$$E_y = \tilde{E}_y(0)\left[\theta(-x)e^{q_- x} + \theta(x)e^{-q_+ x}\right]e^{iky-i\omega t}$$

$$B_z = \frac{i\omega}{q_- c}\tilde{E}_y(0)\left[\theta(-x)e^{q_- x} + \theta(x)e^{-q_+ x}\right]e^{iky-i\omega t}$$

$$E_x = ik\tilde{E}_y(0)\left[\theta(-x)\frac{e^{q_- x}}{q_-} - \theta(x)\frac{e^{-q_+ x}}{q_+}\right]e^{iky-i\omega t}$$

$$\delta n_e = \eta_e\delta(x)e^{iky-i\omega t}$$

Electron surface waves (cold plasma)

Step boundary, overdense plasma:

$n_i = n_0\theta(x)$, $n_0 > 2n_c$

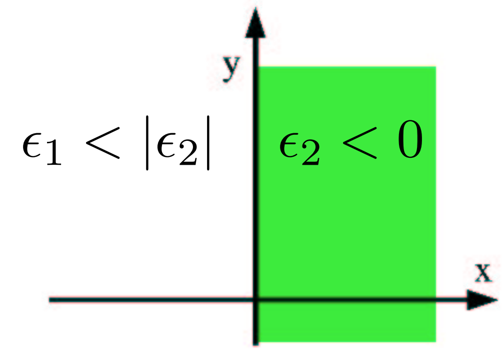

$$E_y = \tilde{E}_y(0)\left[\theta(-x)e^{q_- x} + \theta(x)e^{-q_+ x}\right]e^{iky-i\omega t}$$

$$B_z = \frac{i\omega}{q\_c}\tilde{E}_y(0)\left[\theta(-x)e^{q_- x} + \theta(x)e^{-q_+ x}\right]e^{iky-i\omega t}$$

$$\epsilon_2 = 1 - \frac{\omega_p^2}{\omega^2} = 1 - \frac{n_e}{n_c} < -1$$

$$E_x = ik\tilde{E}_y(0)\left[\theta(-x)\frac{e^{q_- x}}{q_-} - \theta(x)\frac{e^{-q_+ x}}{q_+}\right]e^{iky-i\omega t}$$

$$\delta n_e = \eta_e \delta(x) e^{iky-i\omega t}$$

$$k^2 = \frac{\omega^2}{c^2}\frac{\epsilon_1|\epsilon_2|}{|\epsilon_2| - \epsilon_1} = \frac{\omega^2}{c^2}\frac{\omega_p^2 - \omega^2}{\omega_p^2 - 2\omega^2}$$

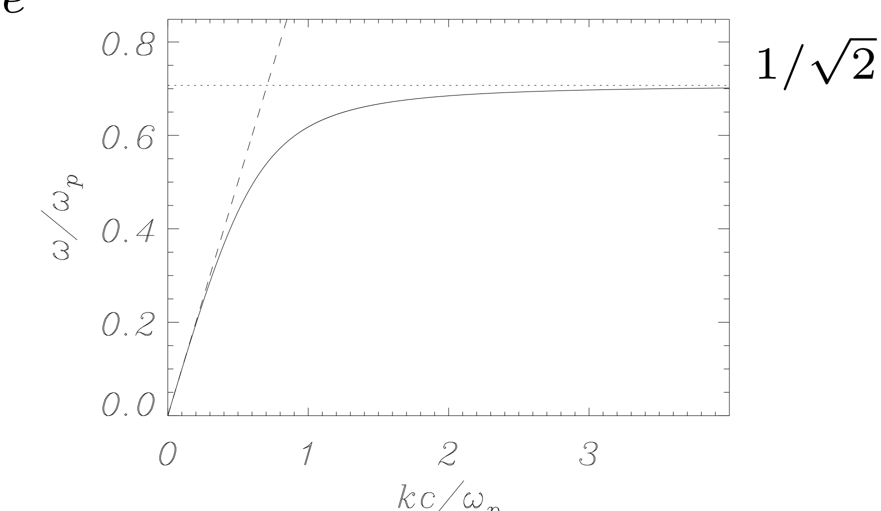

Electron surface waves (warm plasma)

Isothermal closure: $p_e = n_e T_e$, $T_e =$ cost.

Electron surface waves (warm plasma)

Isothermal closure: $p_e = n_e T_e$, $T_e = $ cost.

$$\delta n_e = \delta n_e(0) e^{-\gamma x} e^{iky - i\omega t}$$

$$\gamma = \sqrt{\frac{\omega_p^2 - \omega^2}{v_{th}^2} + k^2}$$

$$\tilde{v}_x = \frac{eE_x}{m_e \omega} \left(e^{-q_+ x} - e^{-\gamma x} \right)$$

(strong shear near $x = 0$)

Electron surface waves (warm plasma)

Isothermal closure: $p_e = n_e T_e$, $T_e =$ cost.

$$\delta n_e = \delta n_e(0) e^{-\gamma x} e^{iky - i\omega t}$$

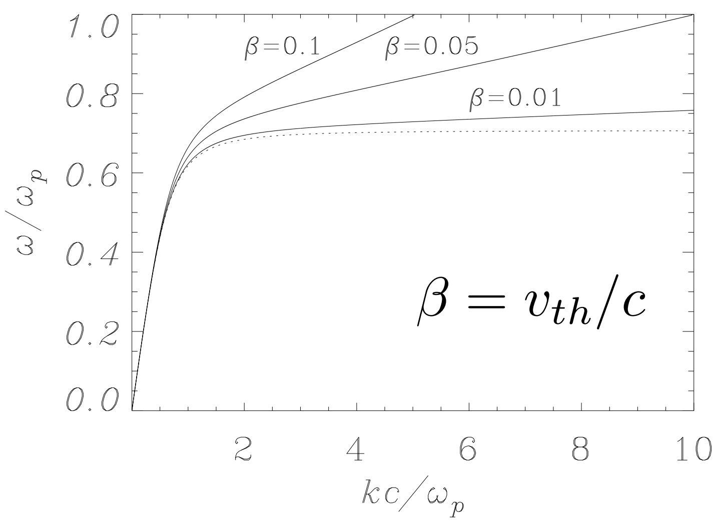

$$\gamma = \sqrt{\frac{\omega_p^2 - \omega^2}{v_{th}^2} + k^2}$$

$$\tilde{v}_x = \frac{eE_x}{m_e \omega} \left(e^{-q_+ x} - e^{-\gamma x} \right)$$

(strong shear near $x = 0$)

For $k \gg \omega/c \longrightarrow \omega^2 \simeq \omega_p^2/2 + k^2 v_{th}^2$

Kaw & Mc Bride, Phys. Fluids **13**, 1784 (1973).

Surface wave absorption : linear case

Linear mode conversion of the laser pulse into a SW at a plane vacuum–plasma interface requires $\omega_L = \omega_s$, $k_L \sin\theta = k_s$ where $k_L = \omega_L/c$ ($L \rightarrow$laser, $s \rightarrow$SW).

Surface wave absorption : linear case

Linear mode conversion of the laser pulse into a SW at a plane vacuum–plasma interface requires $\omega_L = \omega_s$, $k_L \sin\theta = k_s$ where $k_L = \omega_L/c$ $(L \rightarrow$laser, $s \rightarrow$SW).

$\omega_s < k_s c \longrightarrow$ phase matching is *not* possible!

Surface wave absorption : linear case

Linear mode conversion of the laser pulse into a SW at a plane vacuum–plasma interface requires $\omega_L = \omega_s$, $k_L \sin\theta = k_s$ where $k_L = \omega_L/c$ (L $\rightarrow$laser, s $\rightarrow$SW).

$\omega_s < k_s c \longrightarrow$ phase matching is *not* possible!

Structured targets are required, e.g. *grating* targets:

$$k_L \sin\theta = k_s + k_g \qquad (k_g\text{: grating wavevector})$$

Surface wave absorption : linear case

Linear mode conversion of the laser pulse into a SW at a plane vacuum–plasma interface requires $\omega_L = \omega_s$, $k_L \sin\theta = k_s$ where $k_L = \omega_L/c$ ($L \rightarrow$laser, $s \rightarrow$SW).

$\omega_s < k_s c \longrightarrow$ phase matching is *not* possible!

Structured targets are required, e.g. *grating* targets:

$$k_L \sin\theta = k_s + k_g \qquad (k_g\text{: grating wavevector})$$

Peak absorption occurs at optimal incidence angle $\sin\theta = \frac{k_s(\omega_L)+k_g}{\omega_L/c}$

J.-C. Gauthier et al, Proc. SPIE **2523**, 242 (1995)

Surface wave absorption : nonlinear case

In *nonlinear* mode conversion, e.g. a **three-wave process**, phase matching at a planar surface is possible

Surface wave absorption : nonlinear case

In *nonlinear* mode conversion, e.g. a **three-wave process**, phase matching at a planar surface is possible

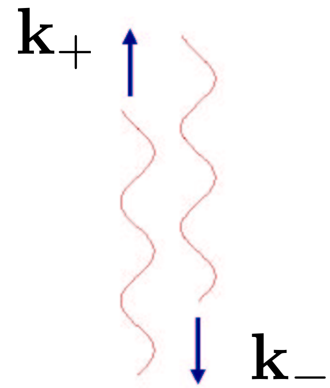

Surface wave absorption : nonlinear case

In *nonlinear* mode conversion, e.g. a **three-wave process**, phase matching at a planar surface is possible

$$\omega_0 = \omega_+ + \omega_-$$
$$k_0 = k_+ + k_-$$

(*Two-Surface Wave Decay*–TSWD)

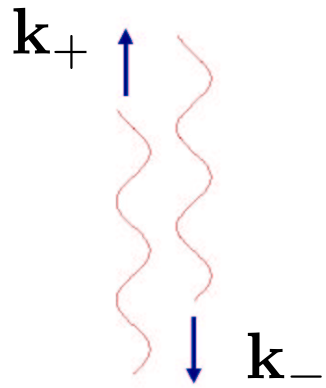

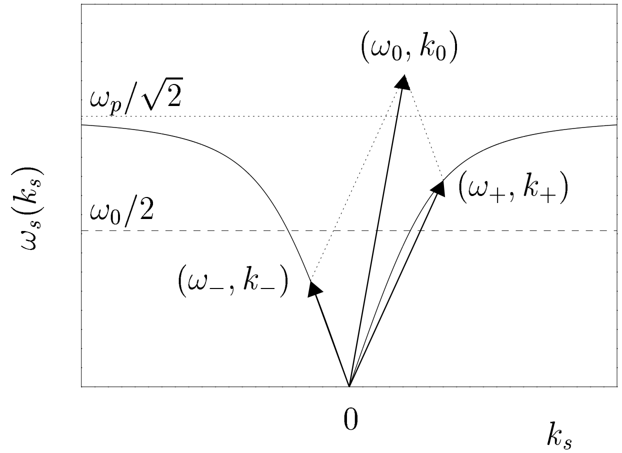

Surface wave absorption : nonlinear case

In *nonlinear* mode conversion, e.g. a **three-wave process**, phase matching at a planar surface is possible

$$\omega_0 = \omega_+ + \omega_-$$
$$k_0 = k_+ + k_-$$

(*Two-Surface Wave Decay*–TSWD)

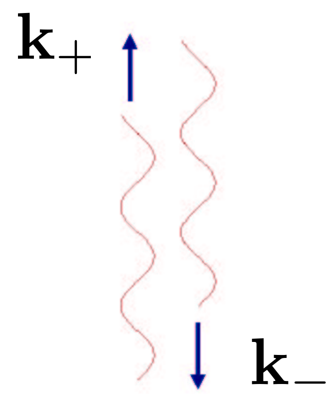

One expects $\omega_0 = \omega_L,\ k_0 = k_L \sin\theta$
$\Longrightarrow \omega_\pm = \omega_0/2 \pm \delta\omega\ \ldots$

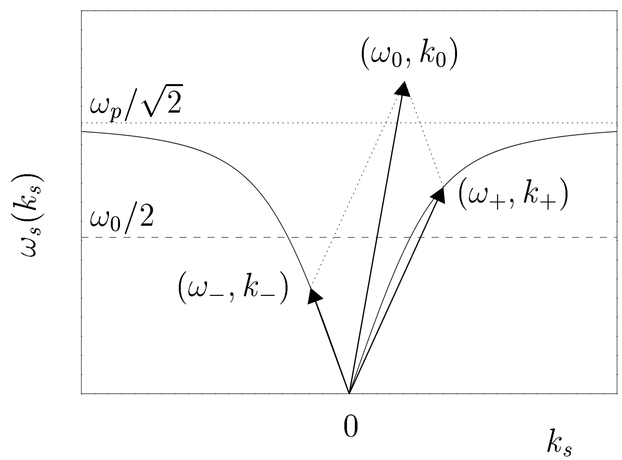

Surface wave absorption : nonlinear case

In *nonlinear* mode conversion, e.g. a **three-wave process**, phase matching at a planar surface is possible

$$\omega_0 = \omega_+ + \omega_-$$
$$k_0 = k_+ + k_-$$

(*Two-Surface Wave Decay*–TSWD)

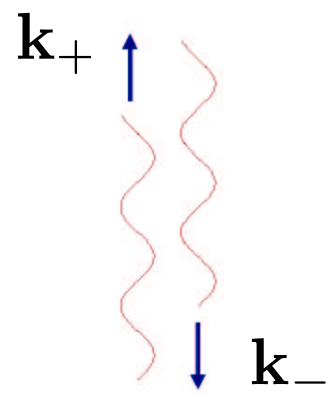

One expects $\omega_0 = \omega_L,\ k_0 = k_L \sin\theta$
$\Longrightarrow \omega_\pm = \omega_0/2 \pm \delta\omega\ \ldots$
... *see later*

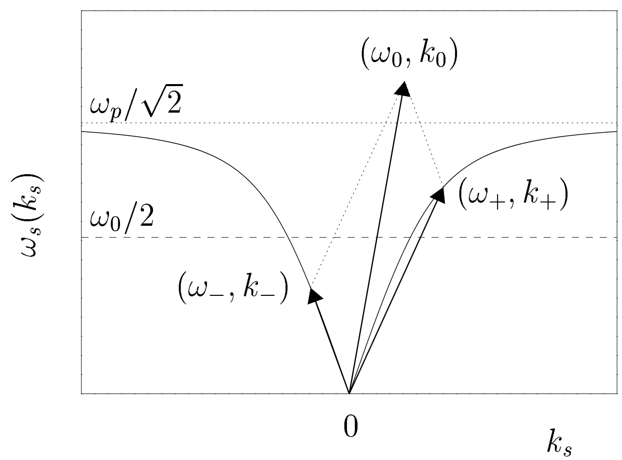

Previous investigations: electrostatic limit ($\omega_s \simeq \omega_p/\sqrt{2}$), different regimes:
Gradov & Stenflo, Phys. Lett. **83A**, 257 (1981);
Stenflo, Phys. Scripta **T63**, 59 (1996).

Search for surface instabilities: early motivations I

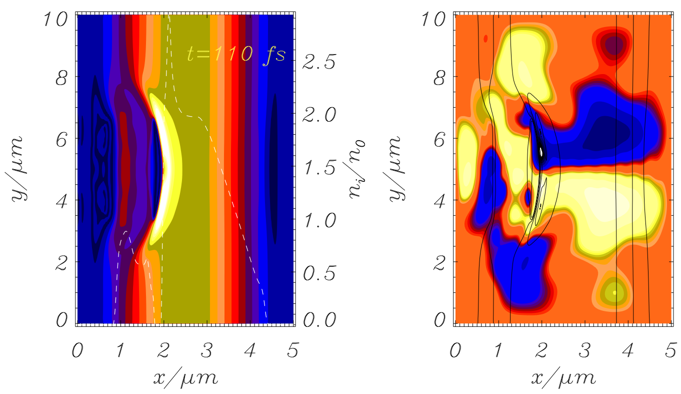

Surface deformations (either dynamic or static) lead to increased absorption and collimate fast electrons

Search for surface instabilities: early motivations I

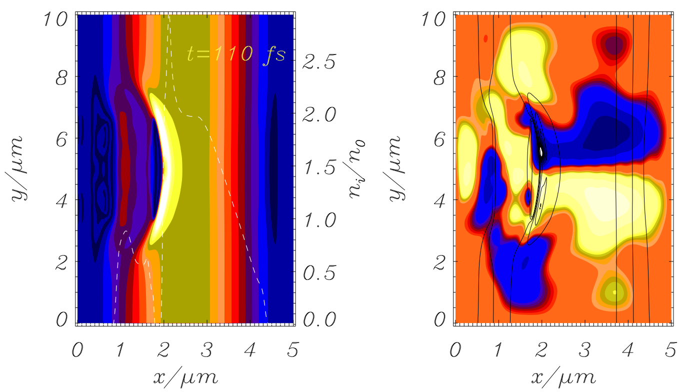

Surface deformations (either dynamic or static) lead to increased absorption and collimate fast electrons ("funnel effect")

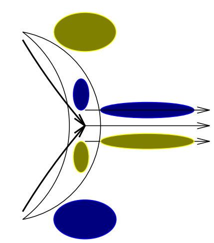

2D Vlasov simulations

Ruhl et al PRL **82**, 2095 (1999)

Search for surface instabilities: early motivations I

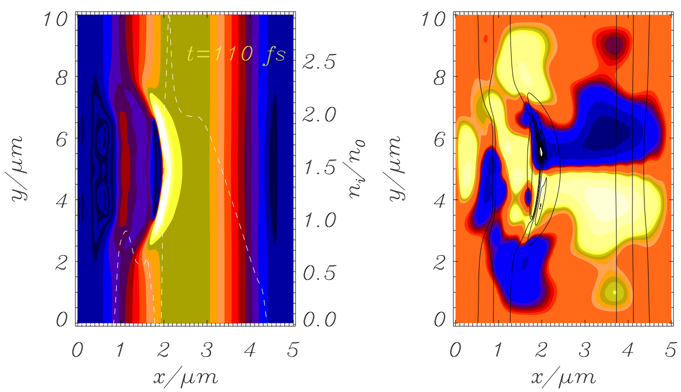

Surface deformations (either dynamic or static) lead to increased absorption and collimate fast electrons (“funnel effect”)

2D Vlasov simulations

Ruhl et al PRL **82**, 2095 (1999)

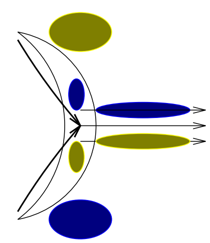

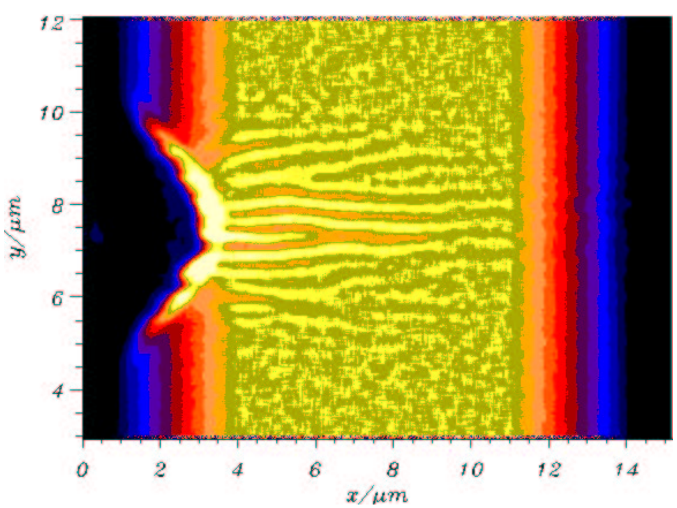

High intensities: surface rippling, multiple electron jets

Search for surface instabilities: early motivations I

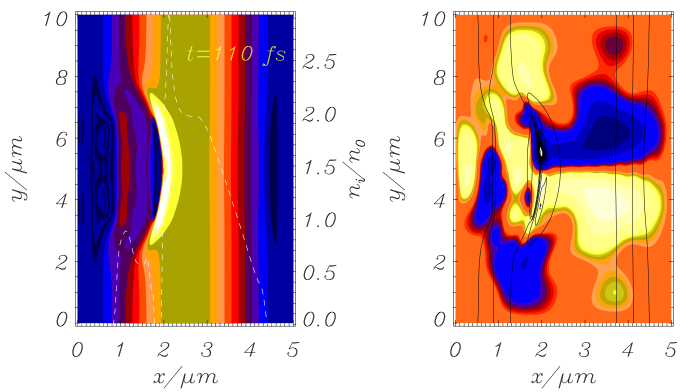

Surface deformations (either dynamic or static) lead to increased absorption and collimate fast electrons ("funnel effect")

2D Vlasov simulations

Ruhl et al PRL **82**, 2095 (1999)

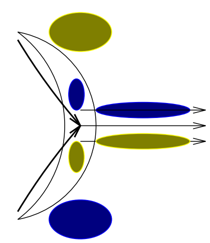

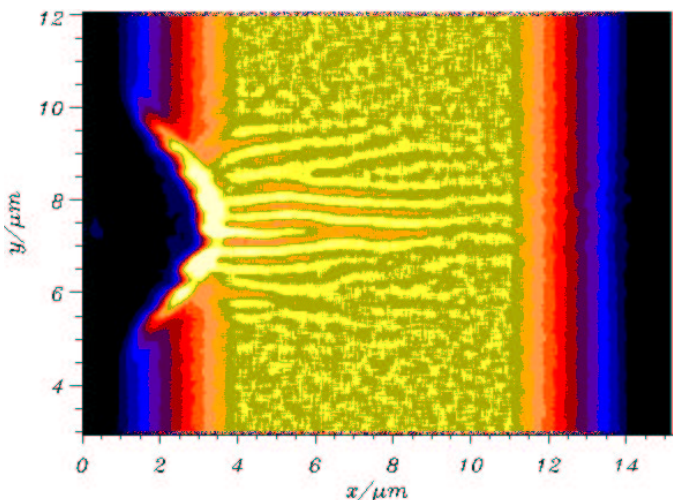

High intensities: surface rippling, multiple electron jets

Vlasov: Macchi et al, LPB **18**, 375 (2000).

PIC: Mulser et al, Las. Phys. **10**, 231 (2000)

Search for surface instabilities: early motivations II

Experiments at high intensity show the onset of surface corrugations in a very short time (≤ 30 fs)

Search for surface instabilities: early motivations II

Experiments at high intensity show the onset of surface corrugations in a very short time (≤ 30 fs)
$\Longrightarrow$ *the mechanism must be of electronic nature*
(ion motion is negligible, hydrodynamic instabilites are ruled out).

Search for surface instabilities: early motivations II

Experiments at high intensity show the onset of surface corrugations in a very short time (≤ 30 fs)
$\Longrightarrow$ *the mechanism must be of electronic nature*
(ion motion is negligible, hydrodynamic instabilites are ruled out).
The effect is detrimental to high harmonic generation from solid surfaces. ("*moving mirror*" effect).

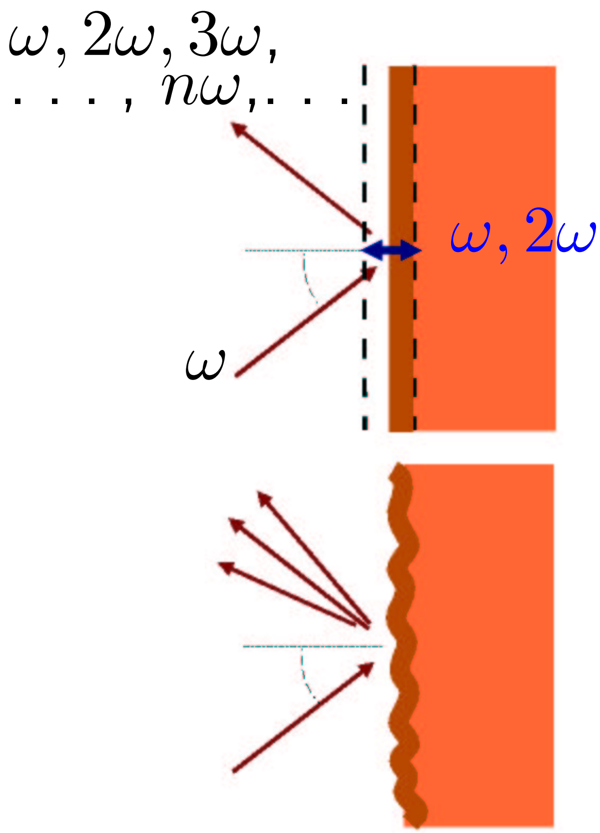

Numerical observations I

2D PIC simulations

- planar geometry
- normal incidence
- s–polarization
- $n_e/n_c = 5$, $a_0 = 1.7$

$(4 \times 10^{18}$ W μm^2 cm$^{-2})$.

Numerical observations I

2D PIC simulations
- planar geometry
- normal incidence
- s–polarization
- $n_e/n_c = 5$, $a_0 = 1.7$

(4×10^{18} W μm^2 cm^{-2}).

n_e/n_c

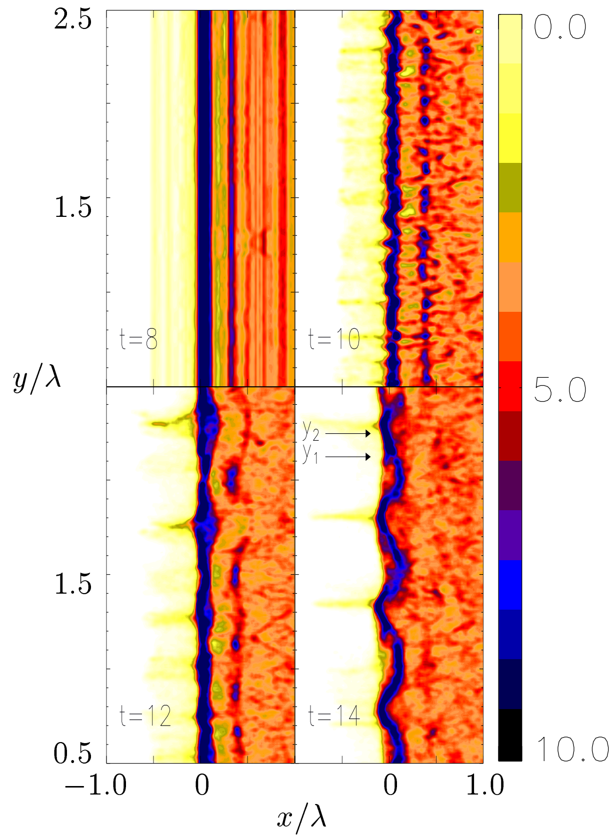

Numerical observations I

2D PIC simulations
- planar geometry
- normal incidence
- s–polarization
- $n_e/n_c = 5$, $a_0 = 1.7$

$(4 \times 10^{18}$ W μm^2 cm$^{-2})$.

Early times: planar (1D) surface motion at 2ω (push–pull by the "$\mathbf{v} \times \mathbf{B}$" force).

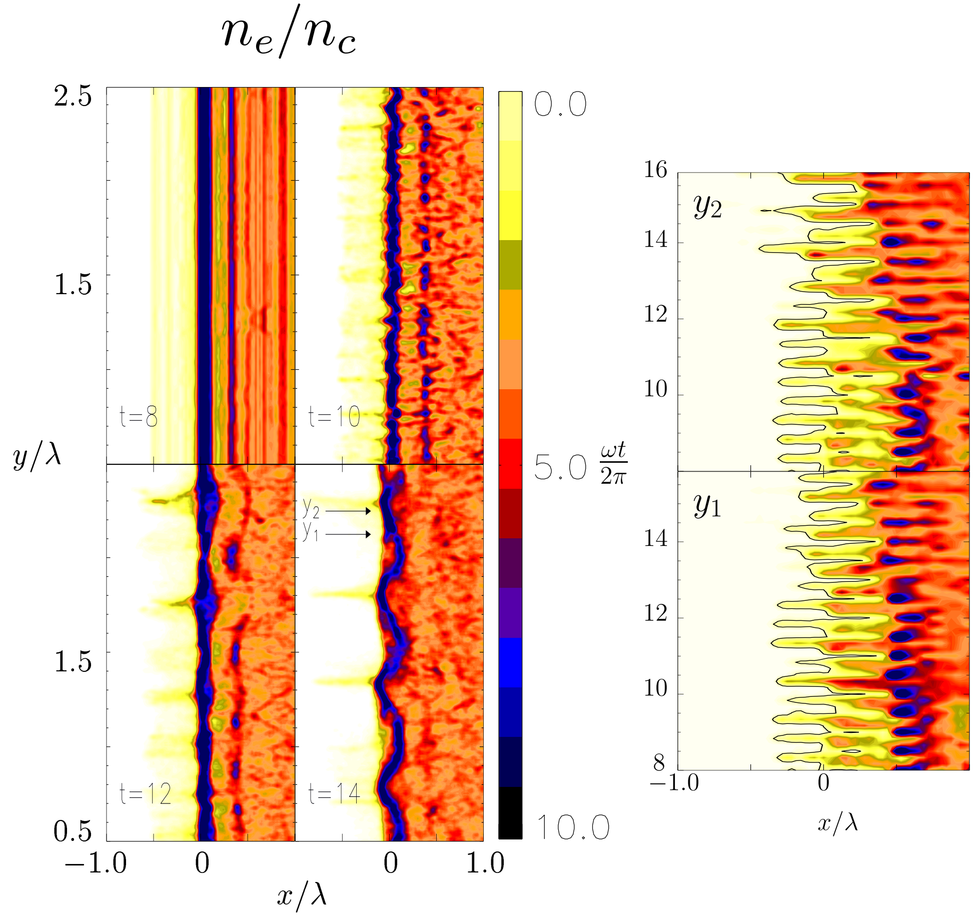

Numerical observations I

2D PIC simulations

- planar geometry
- normal incidence
- s–polarization
- $n_e/n_c = 5$, $a_0 = 1.7$

$(4 \times 10^{18}$ W μm^2 cm$^{-2})$.

Early times: planar (1D) surface motion at 2ω (push–pull by the "$\mathbf{v} \times \mathbf{B}$" force).

Late times: 2D standing surface oscillation (ripples)

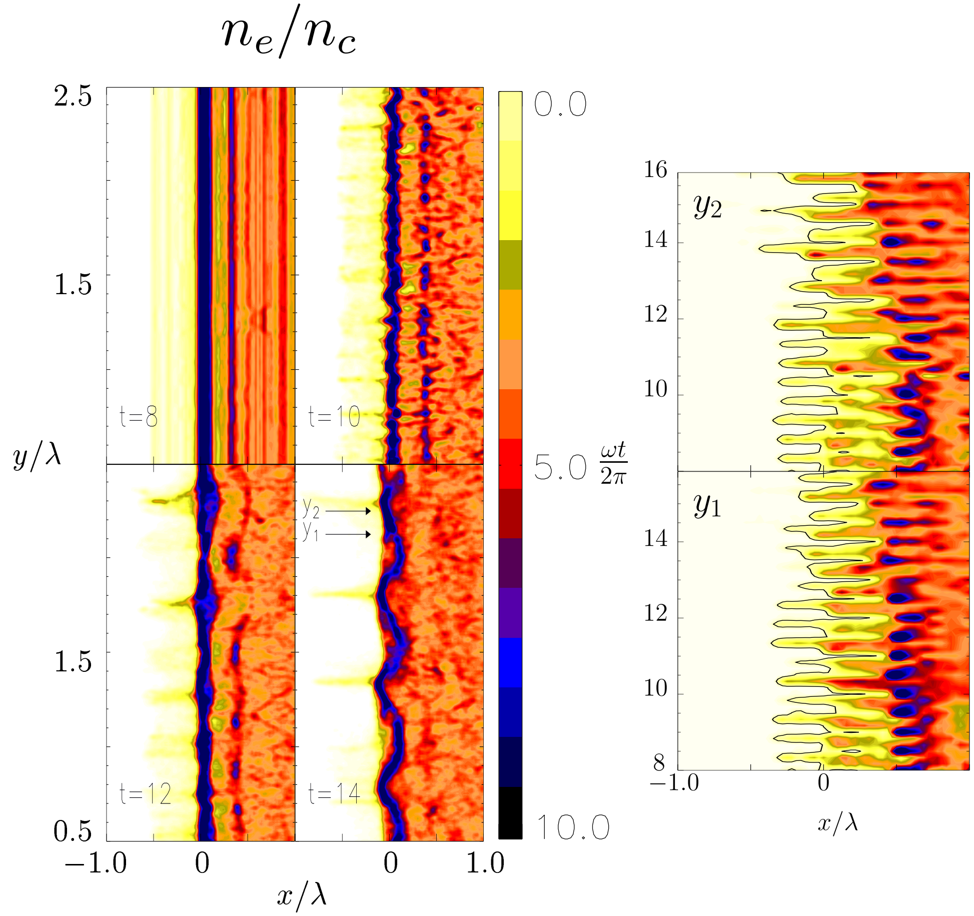

Numerical observations I

2D PIC simulations
- planar geometry
- normal incidence
- s–polarization
- $n_e/n_c = 5$, $a_0 = 1.7$

$(4 \times 10^{18}$ W μm^2 cm^{-2}).

Early times: planar (1D) surface motion at 2ω (push–pull by the "$\mathbf{v} \times \mathbf{B}$" force).

Late times: 2D standing surface oscillation (ripples) *oscillating* at frequency ω ("period doubling").

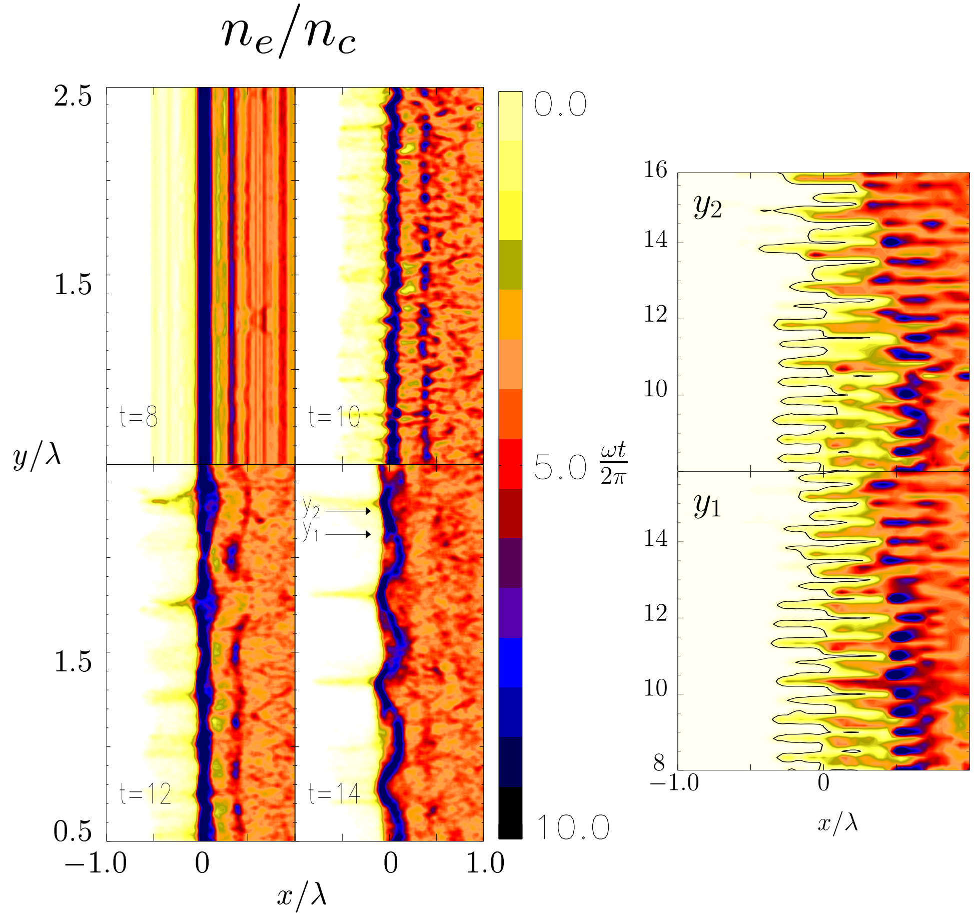

Numerical observations I

2D PIC simulations

- planar geometry
- normal incidence
- s–polarization
- $n_e/n_c = 5$, $a_0 = 1.7$

$(4 \times 10^{18}$ W μm^2 cm$^{-2})$.

Early times: planar (1D) surface motion at 2ω (push–pull by the "$\mathbf{v} \times \mathbf{B}$" force).

Late times: 2D standing surface oscillation (ripples) *oscillating* at frequency ω ("period doubling").

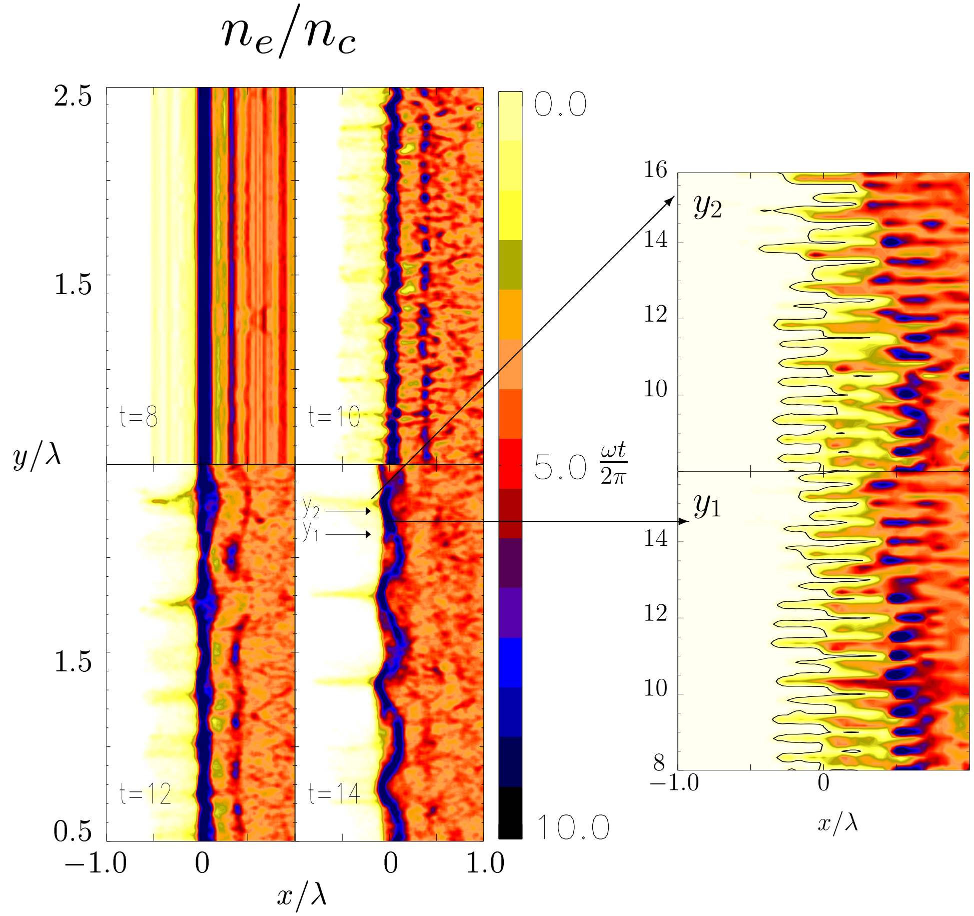

Numerical observations I

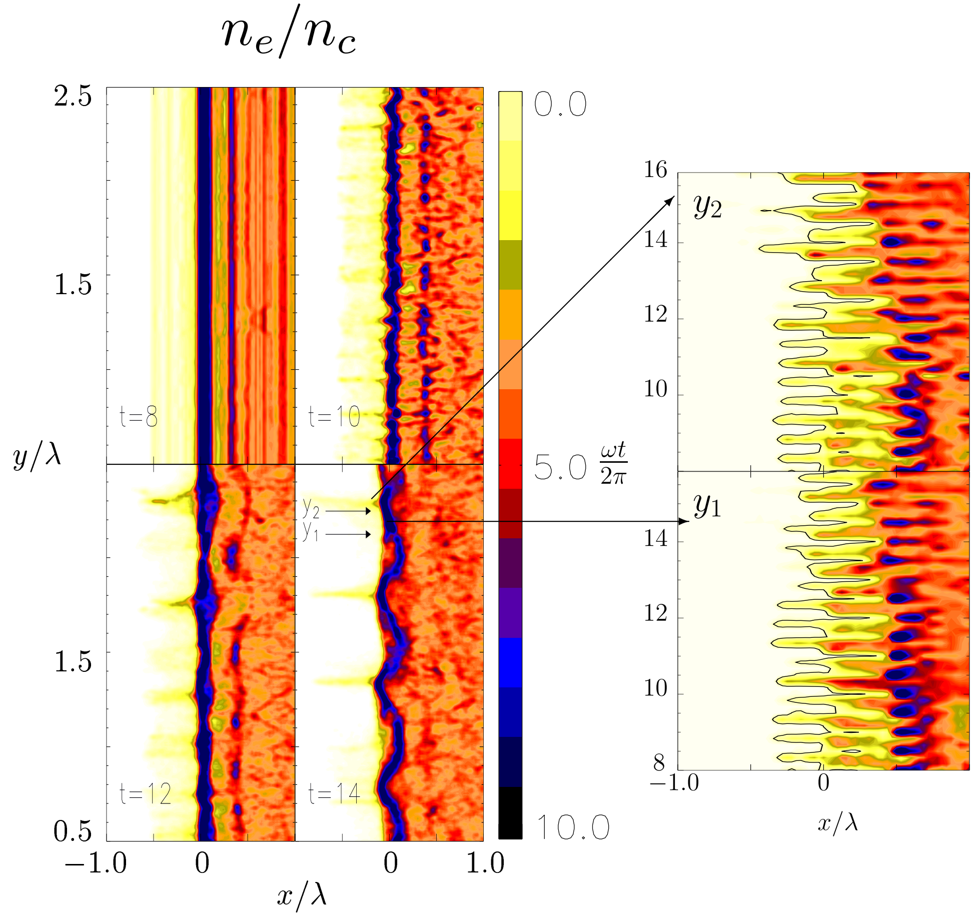

2D PIC simulations

- planar geometry
- normal incidence
- s–polarization
- $n_e/n_c = 5$, $a_0 = 1.7$

(4×10^{18} W μm^2 cm^{-2}).

Early times: planar (1D) surface motion at 2ω (push–pull by the "$\mathbf{v} \times \mathbf{B}$" force).

Late times: 2D standing surface oscillation (ripples)*oscillating* at frequency ω ("period doubling").

A. Macchi et al, PRL **87**, 205004 (2001)

Numerical observations II

At lower intensity ($a_0 = 0.85$) there is no strong rippling but still a period–doubled oscillation: "snaking" of the plasma surface.

Numerical observations II

At lower intensity ($a_0 = 0.85$) there is no strong rippling but still a period–doubled oscillation: "snaking" of the plasma surface.

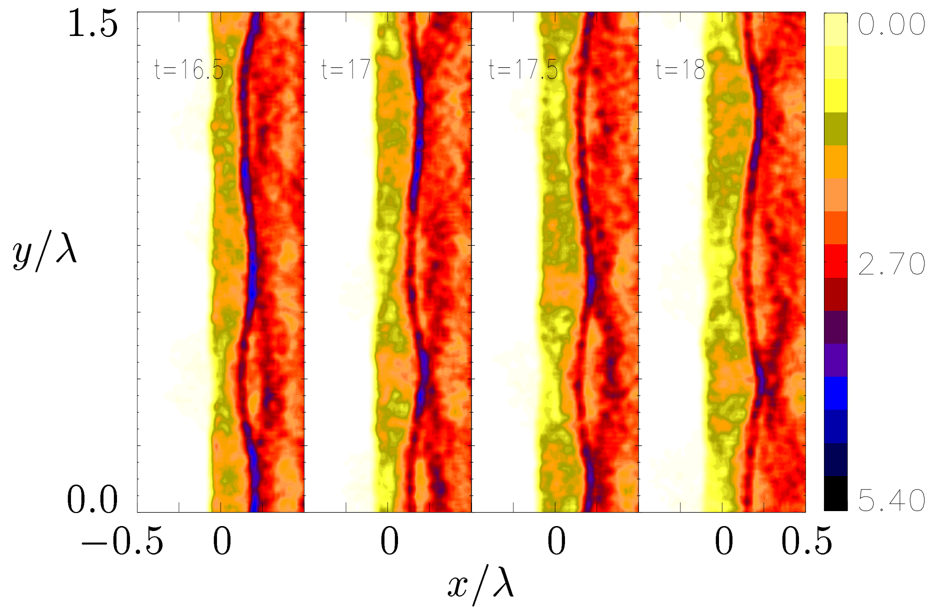

A. Macchi et al, PRL **87**, 205004 (2001)

Numerical observations III

For p-polarization, the quiver motion along y overlaps with the 2D surface oscillation at the same frequency: “ringlet” structures appear
($a_0 = 1.2$)

Numerical observations III

For p-polarization, the quiver motion along y overlaps with the 2D surface oscillation at the same frequency: “ringlet” structures appear
$(a_0 = 1.2)$

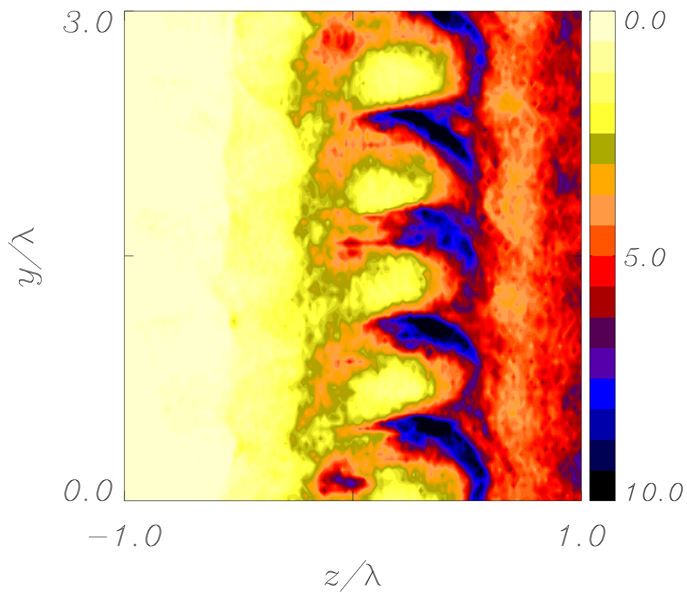

Interpretation: evidence of a parametric process

- Let the $\mathbf{v} \times \mathbf{B}$–driven 1D oscillation be the "pump" mode: $\omega_0 = 2\omega,\ k_0 = 0$.

Interpretation: evidence of a parametric process

- Let the $\mathbf{v} \times \mathbf{B}$–driven 1D oscillation be the "pump" mode: $\omega_0 = 2\omega,\ k_0 = 0$.

- Phase matching conditions for three–wave process: $\omega_0 = \omega_1 + \omega_2 = 2\omega$, $k_0 = k_1 + k_2 = 0 \Rightarrow k_1 = -k_2$.

Interpretation: evidence of a parametric process

- Let the $\mathbf{v} \times \mathbf{B}$–driven 1D oscillation be the "pump" mode: $\omega_0 = 2\omega,\ k_0 = 0$.

- Phase matching conditions for three–wave process: $\omega_0 = \omega_1 + \omega_2 = 2\omega,\ k_0 = k_1 + k_2 = 0 \Rightarrow k_1 = -k_2$.

- Invariance for spatial translation/inversion along y imposes $\omega(k) = \omega(-k)$ for surface modes $\Rightarrow \omega_1 = \omega_2 = \omega_0/2 = \omega$.

Interpretation: evidence of a parametric process

- Let the $\mathbf{v} \times \mathbf{B}$–driven 1D oscillation be the "pump" mode: $\omega_0 = 2\omega,\ k_0 = 0$.
- Phase matching conditions for three–wave process: $\omega_0 = \omega_1 + \omega_2 = 2\omega,\ k_0 = k_1 + k_2 = 0 \Rightarrow k_1 = -k_2$.
- Invariance for spatial translation/inversion along y imposes $\omega(k) = \omega(-k)$ for surface modes $\Rightarrow \omega_1 = \omega_2 = \omega_0/2 = \omega$.
- Overlap of the two excited modes (k, ω) and $(-k, \omega)$ produces a *standing wave* as observed in simulations.

Are the excited modes surface waves ?

- Following quasi-linear, perturbative theory the excited waves must be *normal modes* of the plasma: *electron surface waves* (ESW).

Are the excited modes surface waves ?

- Following quasi-linear, perturbative theory the excited waves must be *normal modes* of the plasma: *electron surface waves* (ESW).

- The observed wavelength of surface modes agrees well with that expected for ESW at moderate intensity, weak density perturbations (i.e. perturbative regime):

Are the excited modes surface waves ?

- Following quasi-linear, perturbative theory the excited waves must be *normal modes* of the plasma: *electron surface waves* (ESW).

- The observed wavelength of surface modes agrees well with that expected for ESW at moderate intensity, weak density perturbations (i.e. perturbative regime):
  (theory: $\lambda_s = 0.71\lambda_L$, simulation: $\lambda_s \approx 0.75\lambda_L$)

Are the excited modes surface waves ?

- Following quasi-linear, perturbative theory the excited waves must be *normal modes* of the plasma: *electron surface waves* (ESW).

- The observed wavelength of surface modes agrees well with that expected for ESW at moderate intensity, weak density perturbations (i.e. perturbative regime):
(theory: $\lambda_s = 0.71\lambda_L$, simulation: $\lambda_s \approx 0.75\lambda_L$)

- The agreement is not good at high (relativistic) intensity, strong density perturbations; the regime is strongly nonlinear

Are the excited modes surface waves ?

- Following quasi-linear, perturbative theory the excited waves must be *normal modes* of the plasma: *electron surface waves* (ESW).

- The observed wavelength of surface modes agrees well with that expected for ESW at moderate intensity, weak density perturbations (i.e. perturbative regime):
  (theory: $\lambda_s = 0.71\lambda_L$, simulation: $\lambda_s \approx 0.75\lambda_L$)

- The agreement is not good at high (relativistic) intensity, strong density perturbations; the regime is strongly nonlinear
  (theory: $\lambda_s = 0.87\lambda_L$, simulation: $\lambda_s \approx 0.5\lambda_L$)

Are the excited modes surface waves ?

- Following quasi-linear, perturbative theory the excited waves must be *normal modes* of the plasma: *electron surface waves* (ESW).

- The observed wavelength of surface modes agrees well with that expected for ESW at moderate intensity, weak density perturbations (i.e. perturbative regime):
  (theory: $\lambda_s = 0.71\lambda_L$, simulation: $\lambda_s \approx 0.75\lambda_L$)

- The agreement is not good at high (relativistic) intensity, strong density perturbations; the regime is strongly nonlinear
  (theory: $\lambda_s = 0.87\lambda_L$, simulation: $\lambda_s \approx 0.5\lambda_L$)
  (hint: if $\omega_p \rightarrow \omega_p/\sqrt{\gamma_0}$, $\lambda_s \rightarrow 0.55\lambda_L$)

Early Numerical Observations in Deformed Targets

Although TSWD does *not* require a grating target, at normal incidence the grating wavevector is equal to that of the resonant SWs: *seeding of TSWD*

Early Numerical Observations in Deformed Targets

Although TSWD does *not* require a grating target, at normal incidence the grating wavevector is equal to that of the resonant SWs: *seeding of TSWD*

Simulations by J. C. Adam for Serena Bastiani's PhD Thesis, Ecole Polytechnique, 1999
$I = 10^{16}$W/cm^2,
$n_e = 10 n_c$, $t = 35$ fs

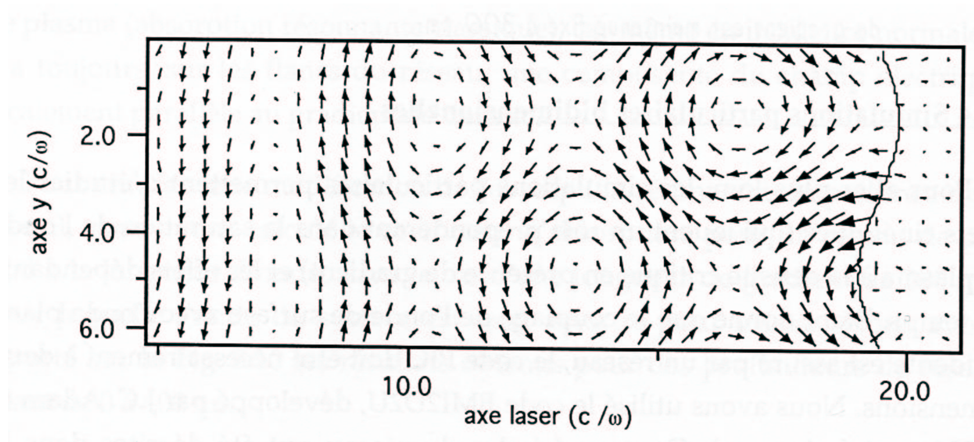

Early Numerical Observations in Deformed Targets

Although TSWD does *not* require a grating target, at normal incidence the grating wavevector is equal to that of the resonant SWs: *seeding of TSWD*

Simulations by J. C. Adam for Serena Bastiani's PhD Thesis, Ecole Polytechnique, 1999
$I = 10^{16}$W/cm^2,
$n_e = 10 n_c$, $t = 35$ fs

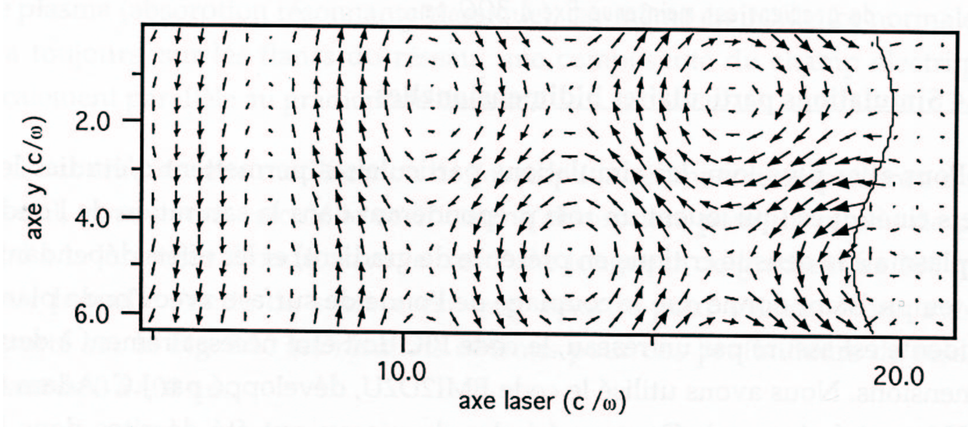

"La disposition des champs s'explique par l'interférence entre le faisceau incident et deux ondes de surface qui se propagent symétriquement le long de la surface."

Analytical theory

Model: *fluid*, non-relativistic, *quasi-linear* perturbative expansion:

$$F(x,y,t) = F_i(x) + \epsilon F_0(x, t - y\sin\theta/c) + \epsilon^2[f_+(x,y,t) + f_-(x,y,t)]$$

ϵ: expansion parameter, $F_0 = \Re\left[\tilde{F}_0(x)e^{-i\omega_0(t-y\sin\theta/c)}\right]$: pump field,
$f_\pm = \Re\left[\tilde{f}_\pm(x)e^{ik_\pm y - i\omega_\pm t}\right]$: SW field

Analytical theory

Model: *fluid*, non-relativistic, *quasi-linear* perturbative expansion:

$$F(x,y,t) = F_i(x) + \epsilon F_0(x, t - y\sin\theta/c) + \epsilon^2[f_+(x,y,t) + f_-(x,y,t)]$$

ϵ: expansion parameter, $F_0 = \Re\left[\tilde{F}_0(x)e^{-i\omega_0(t-y\sin\theta/c)}\right]$: pump field,
$f_\pm = \Re\left[\tilde{f}_\pm(x)e^{ik_\pm y - i\omega_\pm t}\right]$: SW field

Nonlinear coupling force and current with phase $(\omega_\pm, k_\pm)$:

$$\begin{aligned}\mathbf{f}_\pm^{(NL)} = \tilde{\mathbf{f}}_\pm^{(NL)}(x)e^{ik_\pm y - i\omega_\pm t} &= -\epsilon^3 \left[m_e(\mathbf{v}_\mp \cdot \nabla \mathbf{v}_0 + \mathbf{v}_0 \cdot \nabla \mathbf{v}_\mp)\right. \\ &\left. + \frac{e}{c}(\mathbf{v}_0 \times \mathbf{B}_\mp + \mathbf{v} \times \mathbf{B}_0) + \frac{T_e}{n_i^2}\nabla(n_0 n_\mp)\right]_{res}.\end{aligned}$$

Analytical theory

Model: *fluid*, non-relativistic, *quasi-linear* perturbative expansion:

$$F(x,y,t) = F_i(x) + \epsilon F_0(x, t - y\sin\theta/c) + \epsilon^2[f_+(x,y,t) + f_-(x,y,t)]$$

ϵ: expansion parameter, $F_0 = \Re\left[\tilde{F}_0(x)e^{-i\omega_0(t-y\sin\theta/c)}\right]$: pump field,
$f_\pm = \Re\left[\tilde{f}_\pm(x)e^{ik_\pm y - i\omega_\pm t}\right]$: SW field

Nonlinear coupling force and current with phase $(\omega_\pm, k_\pm)$:

$$\begin{aligned}
\mathbf{f}_\pm^{(NL)} = \tilde{\mathbf{f}}_\pm^{(NL)}(x)e^{ik_\pm y - i\omega_\pm t} &= -\epsilon^3\left[m_e(\mathbf{v}_\mp\cdot\nabla\mathbf{v}_0 + \mathbf{v}_0\cdot\nabla\mathbf{v}_\mp)\right. \\
&\left. + \frac{e}{c}(\mathbf{v}_0\times\mathbf{B}_\mp + \mathbf{v}\times\mathbf{B}_0) + \frac{T_e}{n_i^2}\nabla(n_0 n_\mp)\right]_{res}. \\
\mathbf{J}_\pm^{(NL)} = \tilde{\mathbf{J}}_\pm^{(NL)}(x)e^{ik_\pm y - i\omega_\pm t} &= -\left[\epsilon^3 e(n_0\mathbf{v}_\mp + n_\mp\mathbf{v}_0)\right]_{res}
\end{aligned}$$

TSWD channels

The TSWD process is driven by the driven surface oscillation, i.e. by the force component normal to the plasma surface.

TSWD channels

The TSWD process is driven by the driven surface oscillation, i.e. by the force component normal to the plasma surface.

- "$\omega \to \omega/2 + \omega/2$" TSWD:
  $F_x = -eE_x$, oblique incidence,
  $\omega_0 = \omega_L$, $k_0 = k_L \sin\theta$

TSWD channels

The TSWD process is driven by the driven surface oscillation, i.e. by the force component normal to the plasma surface.

- $``\omega \rightarrow \omega/2 + \omega/2''$ TSWD:
  $F_x = -eE_x$, oblique incidence,
  $\omega_0 = \omega_L$, $k_0 = k_L \sin\theta$
  [Macchi et al, Phys. of Plasmas **9**, 1704 (2002)] (cold plasma)

TSWD channels

The TSWD process is driven by the driven surface oscillation, i.e. by the force component normal to the plasma surface.

- "$\omega \to \omega/2 + \omega/2$" TSWD:
  $F_x = -eE_x$, oblique incidence,
  $\omega_0 = \omega_L$, $k_0 = k_L \sin\theta$
  [Macchi et al, Phys. of Plasmas **9**, 1704 (2002)] (cold plasma)

- "$2\omega \to \omega + \omega$" TSWD:
  $F_x = -e(\mathbf{v} \times \mathbf{B})_x$, max. for normal incidence,
  $\omega_0 = 2\omega_L$, $k_0 = 0$

TSWD channels

The TSWD process is driven by the driven surface oscillation, i.e. by the force component normal to the plasma surface.

- "$\omega \to \omega/2 + \omega/2$" TSWD:
  $F_x = -eE_x$, oblique incidence,
  $\omega_0 = \omega_L$, $k_0 = k_L \sin\theta$
  [Macchi et al, Phys. of Plasmas **9**, 1704 (2002)] (cold plasma)

- "$2\omega \to \omega + \omega$" TSWD:
  $F_x = -e(\mathbf{v} \times \mathbf{B})_x$, max. for normal incidence,
  $\omega_0 = 2\omega_L$, $k_0 = 0$

Pump mode for $2\omega \rightarrow \omega + \omega$ TSWD

Pump: electrostatic oscillation driven by $\mathbf{v} \times \mathbf{B}$ force at 2ω along $\hat{\mathbf{x}}$ ($\theta = 0$)

Pump mode for $2\omega \to \omega + \omega$ TSWD

Pump: electrostatic oscillation driven by $\mathbf{v} \times \mathbf{B}$ force at 2ω along $\hat{\mathbf{x}}$ ($\theta = 0$)

$$F_x^{(2\omega)} = \frac{m_e \omega^2}{2 l_s} a^2(0) e^{-2x/l_s - 2i\omega t} \equiv F_0 e^{-2x/l_s - 2i\omega t} \qquad \left(l_s = c/\sqrt{\omega_p^2 - \omega^2} \right)$$

Velocity field amplitude:

$$\tilde{V}_x^{(2\omega)} = \frac{-2i\omega F_0 n_i / m_e}{4\omega^2 - \omega_p^2 - 4 v_{th}^2 / l_s^2} \left(e^{-2x/l_s} - e^{i k_2 x} \right) \qquad \left(k_2 = \sqrt{4\omega^2 - \omega_p^2} / v_{th} \right)$$

Pump mode for $2\omega \rightarrow \omega + \omega$ TSWD

Pump: electrostatic oscillation driven by $\mathbf{v} \times \mathbf{B}$ force at 2ω along $\hat{\mathbf{x}}$ ($\theta = 0$)

$$F_x^{(2\omega)} = \frac{m_e \omega^2}{2l_s} a^2(0) e^{-2x/l_s - 2i\omega t} \equiv F_0 e^{-2x/l_s - 2i\omega t} \qquad \left(l_s = c/\sqrt{\omega_p^2 - \omega^2} \right)$$

Velocity field amplitude:

$$\tilde{V}_x^{(2\omega)} = \frac{-2i\omega F_0 n_i / m_e}{4\omega^2 - \omega_p^2 - 4v_{th}^2/l_s^2} \left(e^{-2x/l_s} - e^{ik_2 x} \right) \qquad (k_2 = \sqrt{4\omega^2 - \omega_p^2}/v_{th})$$

Plasmon resonance at $2\omega = \sqrt{\omega_p^2 + 4v_{th}^2/l_s^2}$

The growth rate

Temporal variation of the SW energy U:

The growth rate

Temporal variation of the SW energy U:

$$\Gamma U_{\pm} \equiv \partial_t U_{\pm} = \quad \frac{2\pi}{k} \int_{-\pi/k}^{+\pi/k} dy \int_0^{\infty} dx \partial_t \langle u_{\pm} \rangle$$

The growth rate

Temporal variation of the SW energy U:

$$\begin{aligned}\Gamma U_{\pm} \equiv \partial_t U_{\pm} = & \quad \frac{2\pi}{k}\int_{-\pi/k}^{+\pi/k} dy \int_0^{\infty} dx \partial_t \langle u_{\pm} \rangle \\ u_{\pm} = & \quad (u_{kin} + u_{EM} + u_{th})_{\pm}\end{aligned}$$

The growth rate

Temporal variation of the SW energy U:

$$\begin{aligned}
\Gamma U_\pm \equiv \partial_t U_\pm = & \quad \frac{2\pi}{k}\int_{-\pi/k}^{+\pi/k} dy \int_0^\infty dx \partial_t \langle u_\pm \rangle \\
u_\pm = & \quad (u_{kin} + u_{EM} + u_{th})_\pm \\
\partial_t \langle u_\pm \rangle = & \quad \left\langle \mathbf{f}_\pm^{(NL)} \cdot \mathbf{v}_\pm - \mathbf{J}_\pm^{(NL)} \cdot \mathbf{E}_\pm \right\rangle
\end{aligned}$$

Including thermal effects is important because in the $T_e = 0$ limit, nonlinear terms such as $V_x^{(\omega_0)} v_{\mp,x} \partial_x v_{\pm,x}$, $n_\pm V_x^{(\omega_0)} v_{\pm,x}$... are singular at $x = 0$.

The growth rate

Temporal variation of the SW energy U:

$$\Gamma U_\pm \equiv \partial_t U_\pm = \frac{2\pi}{k}\int_{-\pi/k}^{+\pi/k} dy \int_0^\infty dx \partial_t \langle u_\pm \rangle$$

$$u_\pm = (u_{kin} + u_{EM} + u_{th})_\pm$$

$$\partial_t \langle u_\pm \rangle = \left\langle \mathbf{f}_\pm^{(NL)} \cdot \mathbf{v}_\pm - \mathbf{J}_\pm^{(NL)} \cdot \mathbf{E}_\pm \right\rangle$$

Including thermal effects is important because in the $T_e = 0$ limit, nonlinear terms such as $V_x^{(\omega_0)} v_{\mp,x} \partial_x v_{\pm,x}$, $n_\pm V_x^{(\omega_0)} v_{\pm,x}$... are singular at $x = 0$.

The spatial singularities are removed by the pressure term.
The "cold" result is thus obtained taking the $T_e \to 0$ limit.

The $2\omega \rightarrow \omega + \omega$ growth rate

Dashed: "cold" case

Macchi et al, PoP **9**, 1704 (2002)

Solid: "hot" case

(labels: thermal velocity v_{th}/c)

M. Battaglini, *laurea* thesis, 2002;

Macchi et al, Appl. Phys. B (2004), submitted.

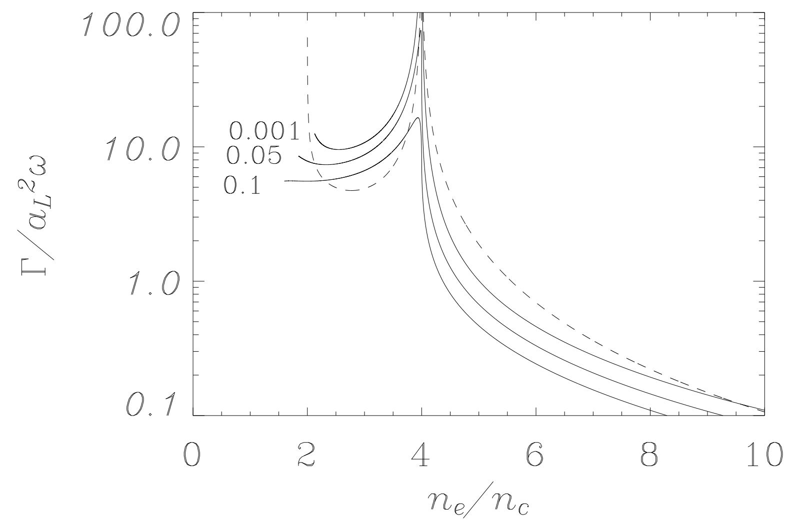

The $2\omega \to \omega + \omega$ growth rate

Dashed: "cold" case

Macchi et al, PoP **9**, 1704 (2002)

Solid: "hot" case

(labels: thermal velocity v_{th}/c)

M. Battaglini, *laurea* thesis, 2002;

Macchi et al, Appl. Phys. B (2004), submitted.

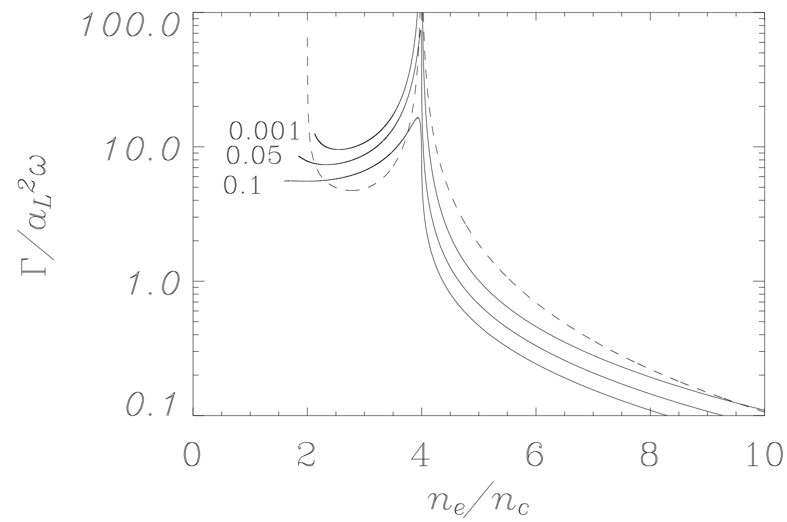

$\omega \to \omega_p/\sqrt{2}$, $k \to \infty$; small scales washed out by thermal effects

The $2\omega \rightarrow \omega + \omega$ growth rate

Dashed: "cold" case

Macchi et al, PoP **9**, 1704 (2002)

Solid: "hot" case

(labels: thermal velocity v_{th}/c)

M. Battaglini, *laurea* thesis, 2002;

Macchi et al, Appl. Phys. B (2004), submitted.

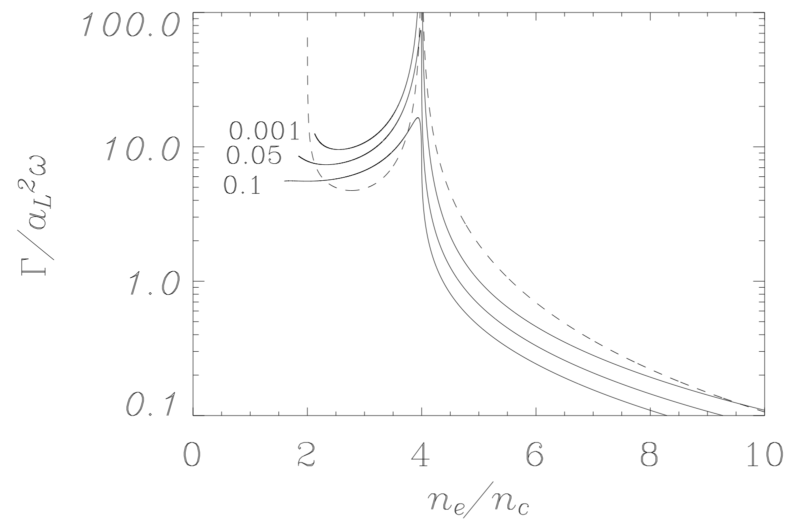

$\omega \rightarrow \omega_p/\sqrt{2}$, $k \rightarrow \infty$; small scales washed out by thermal effects

$\omega = \omega_p/2$; "pump" resonance quenched by plasmon propagation out of the surface

TSWD effects on electron acceleration

- It is known that electron heating at a step laser–plasma interface is
  - due to non–adiabatic motion in evanescent fields

TSWD effects on electron acceleration

- It is known that electron heating at a step laser–plasma interface is
  - due to non–adiabatic motion in evanescent fields
  - dominated by the force component normal to the surface

TSWD effects on electron acceleration

- It is known that electron heating at a step laser–plasma interface is
  - due to non–adiabatic motion in evanescent fields
  - dominated by the force component normal to the surface

- Surface waves excited in "grating" targets affect electron heating

TSWD effects on electron acceleration

- It is known that electron heating at a step laser–plasma interface is
  - due to non–adiabatic motion in evanescent fields
  - dominated by the force component normal to the surface

- Surface waves excited in "grating" targets affect electron heating (C. Riconda et al, to appear in PoP)

TSWD effects on electron acceleration

- It is known that electron heating at a step laser–plasma interface is
  - due to non–adiabatic motion in evanescent fields
  - dominated by the force component normal to the surface

- Surface waves excited in "grating" targets affect electron heating (C. Riconda et al, to appear in PoP)

- How is electron heating affected by a *standing* SW?

TSWD effects on electron acceleration

- It is known that electron heating at a step laser–plasma interface is
  - due to non–adiabatic motion in evanescent fields
  - dominated by the force component normal to the surface

- Surface waves excited in "grating" targets affect electron heating (C. Riconda et al, to appear in PoP)

- How is electron heating affected by a *standing* SW?

$\rightarrow$ We performed **test particle simulations** of electron motion in the pump+SW fields involved in TSWD.

Set–up of test particle simulations

- Force: superposition of 1D “pump” field $\sim \cos 2\omega t$

Set–up of test particle simulations

- Force: superposition of 1D "pump" field $\sim \cos 2\omega t$
  plus 2D standing SW field $\sim \sin \omega t \sin(2\pi y/\lambda_s)$

Set–up of test particle simulations

- Force: superposition of 1D "pump" field $\sim \cos 2\omega t$
  plus 2D standing SW field $\sim \sin \omega t \sin(2\pi y/\lambda_s)$

- Amplitudes: $a_0^{(2\omega)} = 0.2$, $a_0^{(\omega)} = 0.019$

Set–up of test particle simulations

- Force: superposition of 1D "pump" field $\sim \cos 2\omega t$
  plus 2D standing SW field $\sim \sin \omega t \sin(2\pi y/\lambda_s)$
- Amplitudes: $a_0^{(2\omega)} = 0.2$, $a_0^{(\omega)} = 0.019$
- Plasma density: $n_e/n_c = \omega_p^2/\omega^2 = 5$
- Initial spatial distribution: uniform in y over one λ_s length

Set–up of test particle simulations

- Force: superposition of 1D "pump" field $\sim \cos 2\omega t$
  plus 2D standing SW field $\sim \sin \omega t \sin(2\pi y/\lambda_s)$

- Amplitudes: $a_0^{(2\omega)} = 0.2$, $a_0^{(\omega)} = 0.019$

- Plasma density: $n_e/n_c = \omega_p^2/\omega^2 = 5$

- Initial spatial distribution: uniform in y over one λ_s length

- Initial velocity distribution: drifting in x with average $v_x = -0.1$
  (particles move from the plasma towards the surface)

Enhanced acceleration near SW maxima

Top: (y, p_x) phase space projections from PIC simulations at two subsequent times

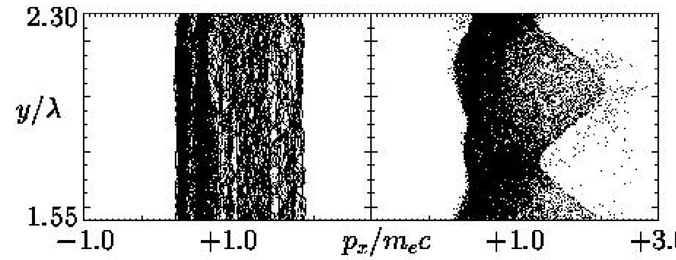

Enhanced acceleration near SW maxima

Top: (y, p_x) phase space projections from PIC simulations at two subsequent times

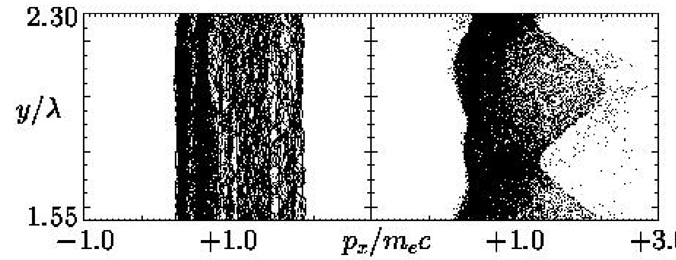

Bottom: same phase space projection from test particle simulations

Enhanced acceleration near SW maxima

Top: (y, p_x) phase space projections from PIC simulations at two subsequent times

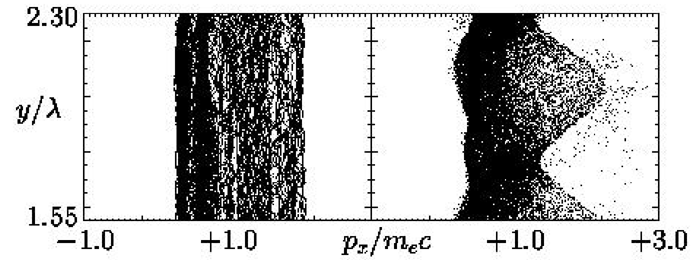

Bottom: same phase space projection from test particle simulations

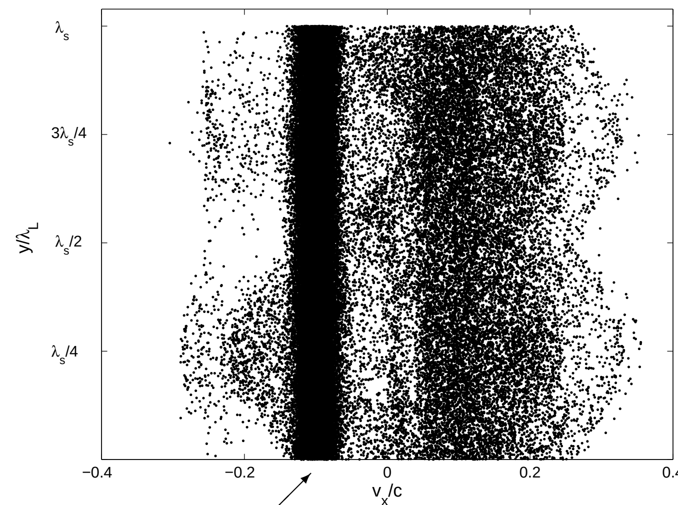

"Black stripe": initial conditions

Enhanced acceleration near SW maxima

Top: (y, p_x) phase space projections from PIC simulations at two subsequent times

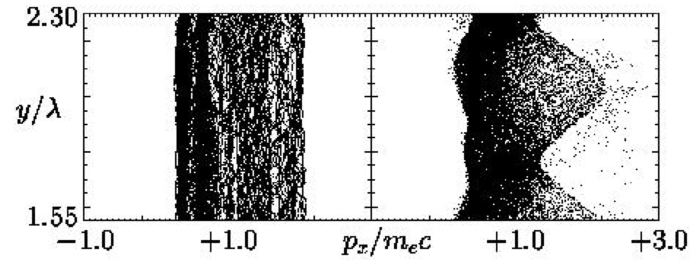

Bottom: same phase space projection from test particle simulations

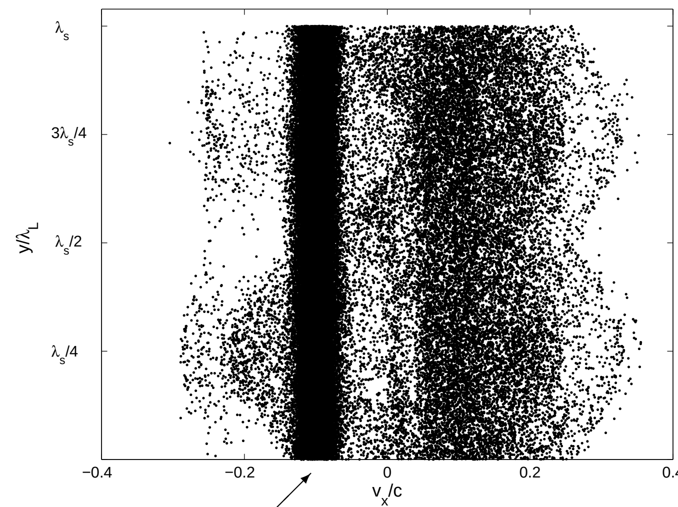

"Black stripe": initial conditions

PIC and test-particle simulations both show enhanced electron heating near SW maxima

Enhanced acceleration near SW maxima

Top: (y, p_x) phase space projections from PIC simulations at two subsequent times

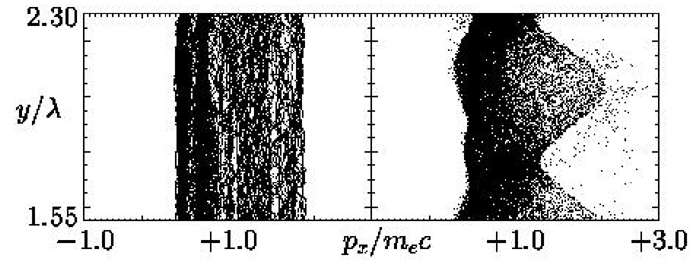

Bottom: same phase space projection from test particle simulations

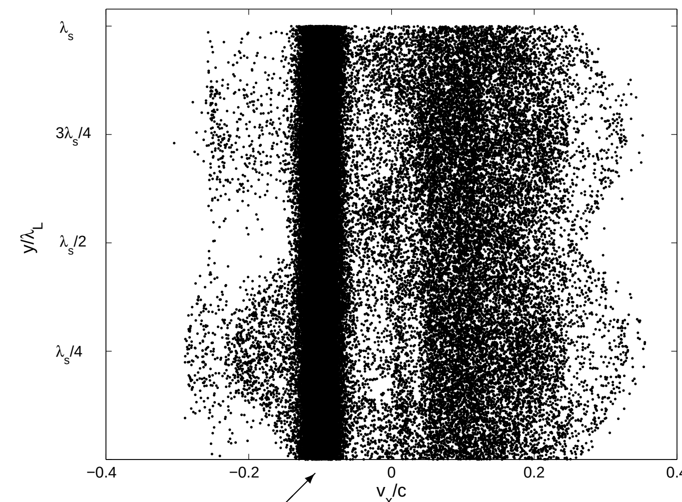

"Black stripe": initial conditions

PIC and test-particle simulations both show enhanced electron heating near SW maxima

A. Macchi et al, Appl. Phys. B, submitted

Enhanced acceleration in time domain

(x, p_x) phase space

Black: all electrons in simulation

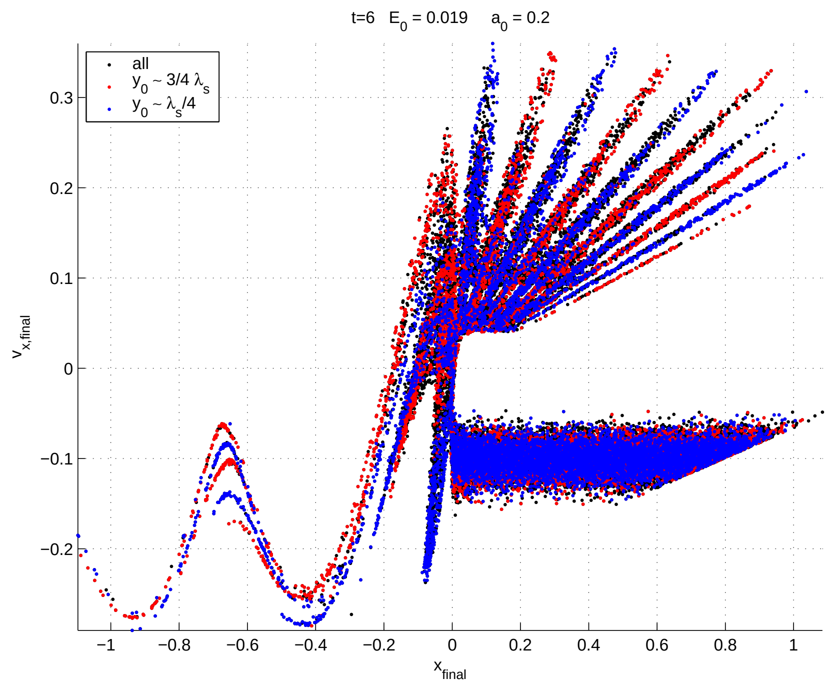

Enhanced acceleration in time domain

(x, p_x) phase space

Black: all electrons in simulation
Blue: electrons starting around $y = \lambda_s/4$

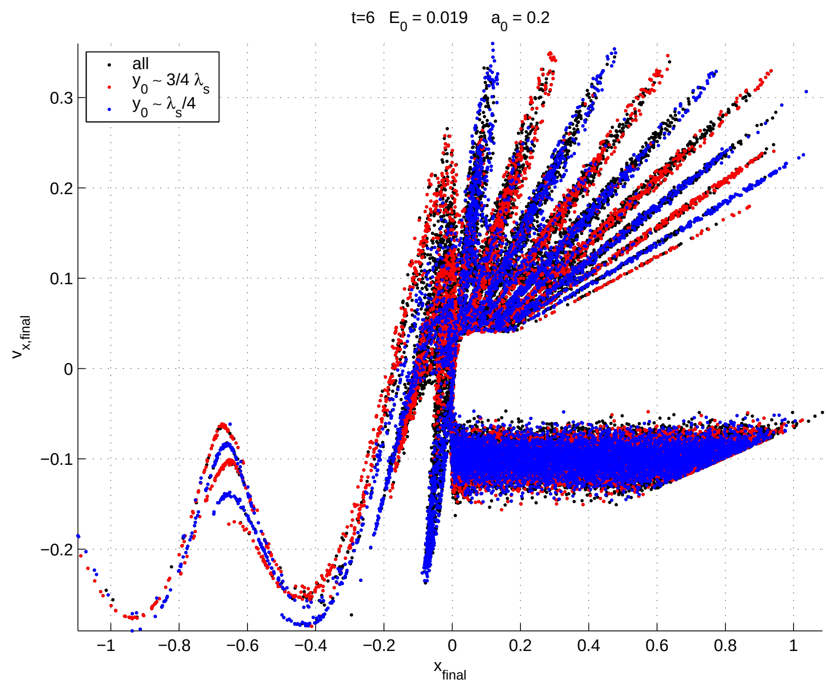

Enhanced acceleration in time domain

(x, p_x) phase space

Black: all electrons in simulation
Blue: electrons starting around $y = \lambda_s/4$
Red: electrons starting around $y = 3\lambda_s/4$

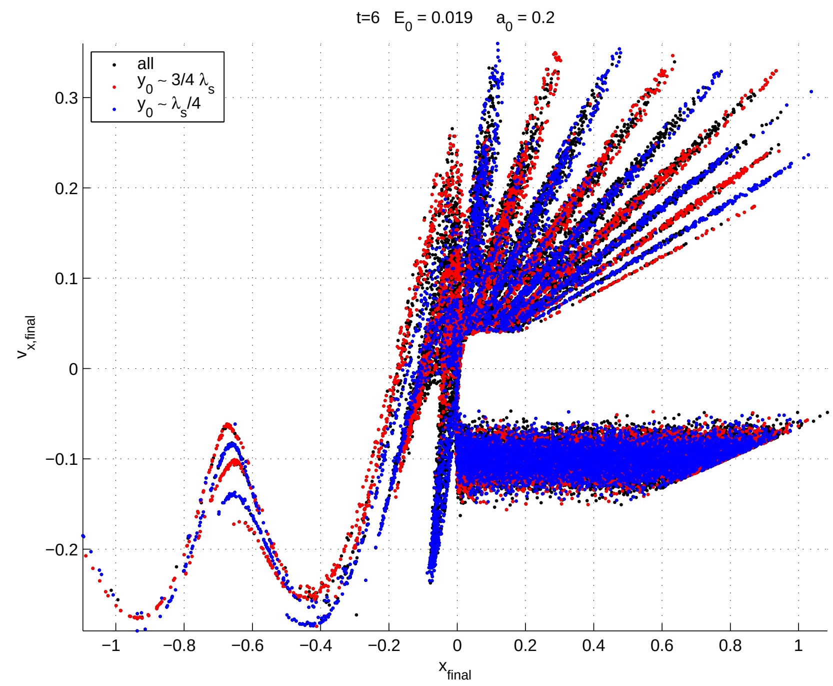

Enhanced acceleration in time domain

(x, p_x) phase space

Black: all electrons in simulation
Blue: electrons starting around $y = \lambda_s/4$
Red: electrons starting around $y = 3\lambda_s/4$

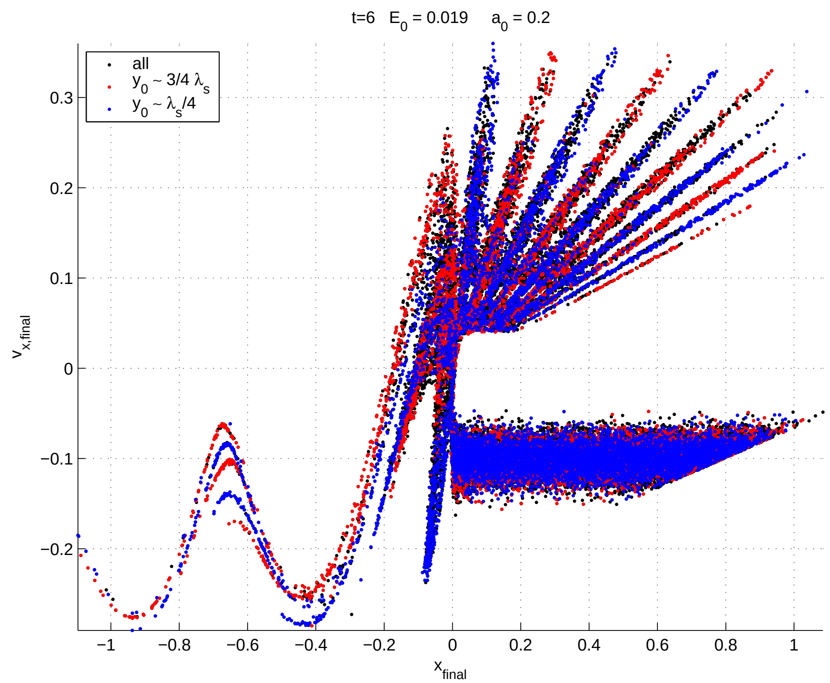

– "Jets" are produced at 2ω rate (by $\mathbf{v} \times \mathbf{B}$ force).

Enhanced acceleration in time domain

(x, p_x) phase space

Black: all electrons in simulation
Blue: electrons starting around $y = \lambda_s/4$
Red: electrons starting around $y = 3\lambda_s/4$

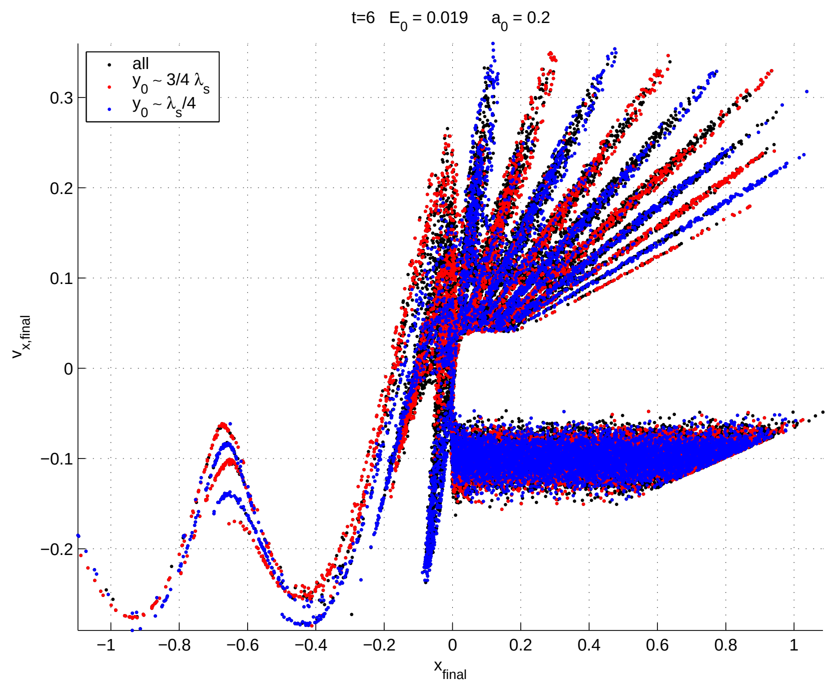

– "Jets" are produced at 2ω rate (by $\mathbf{v} \times \mathbf{B}$ force).

– Enhanced acceleration by SW occurs at ω rate.

Enhanced acceleration in time domain

(x, p_x) phase space

Black: all electrons in simulation
Blue: electrons starting around $y = \lambda_s/4$
Red: electrons starting around $y = 3\lambda_s/4$

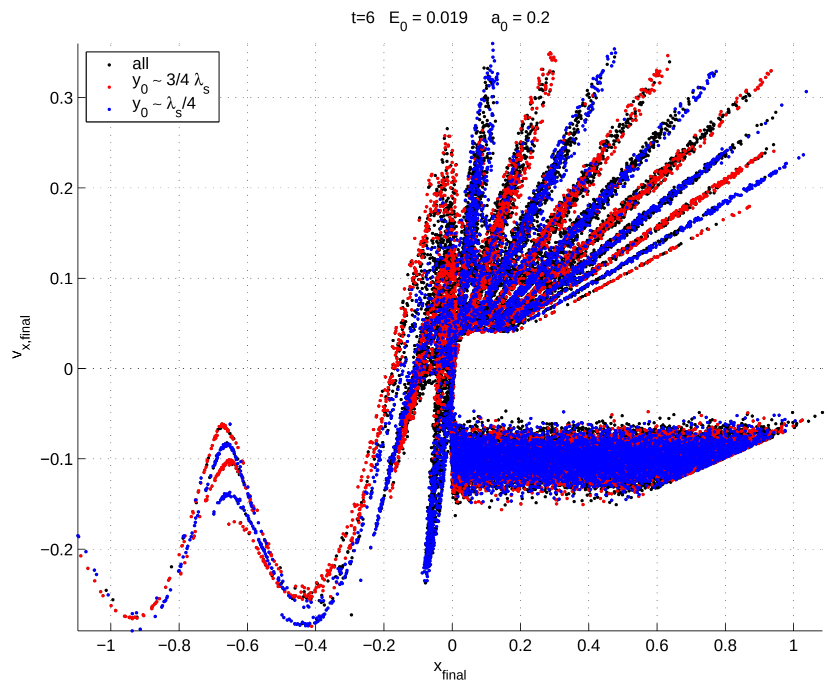

– "Jets" are produced at 2ω rate (by $\mathbf{v} \times \mathbf{B}$ force).

– Enhanced acceleration by SW occurs at ω rate.

– Near SW maxima some electrons are emitted into vacuum $(x < 0)$
(p_x modulated by $\mathbf{v} \times \mathbf{B} \sim \cos 2k_L x$ in vacuum)

Induced modulation of electron current

The electron current density $j_{e,x}$ is reconstructed from test particle phase space.

Induced modulation of electron current

The electron current density $j_{e,x}$ is reconstructed from test particle phase space.

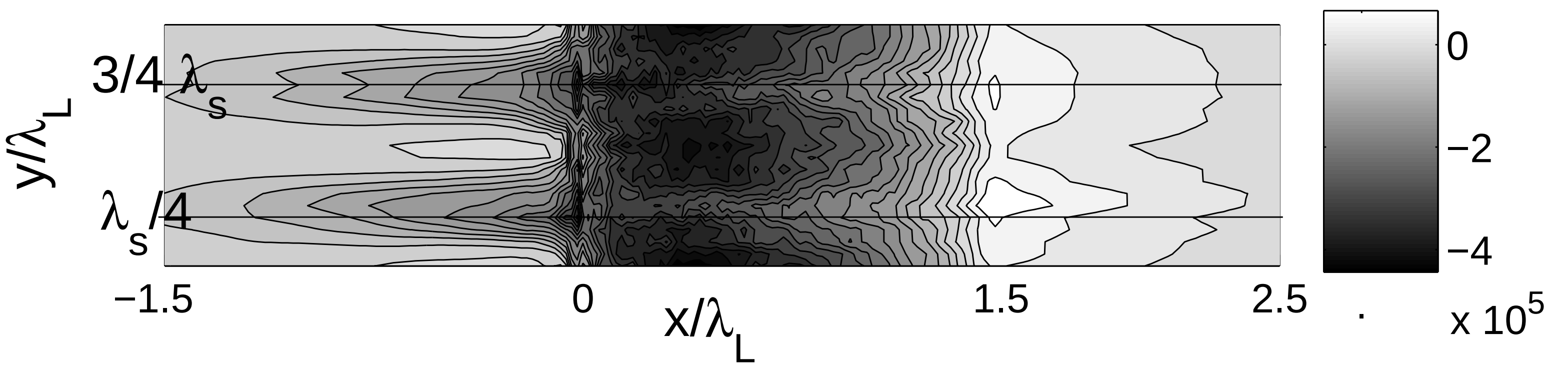

$j_{e,x}$ is spatially modulated in y with the SW periodicity.

Induced modulation of electron current

The electron current density $j_{e,x}$ is reconstructed from test particle phase space.

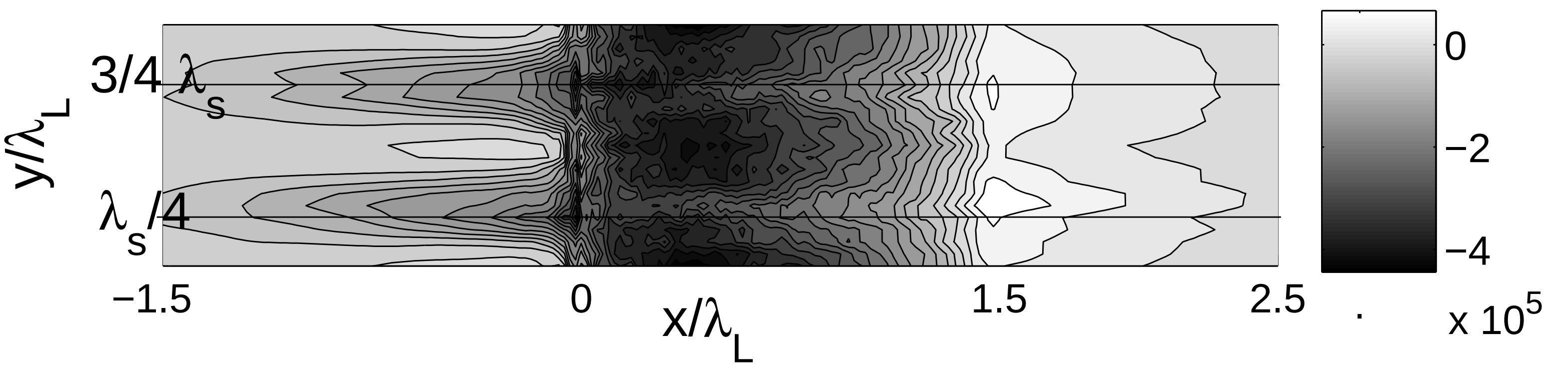

$j_{e,x}$ is spatially modulated in y with the SW periodicity.

Spatial imprint for current filamentation?

Interplay with “Weibel” instabilities?

Linear stability analysis and 3D fluid simulation (F. Califano) show that the relativistic “Weibel” instability of *counterstreaming*, *asymmetrical beams* (e.g. fast electrons current and slow return current) does *not* lead to filaments *unless* the initial beams have finite width (i.e. a given $k_\perp$).

Interplay with "Weibel" instabilities?

Linear stability analysis and 3D fluid simulation (F. Califano) show that the relativistic "Weibel" instability of *counterstreaming*, *asymmetrical beams* (e.g. fast electrons current and slow return current) does *not* lead to filaments *unless* the initial beams have finite width (i.e. a given $k_\perp$).

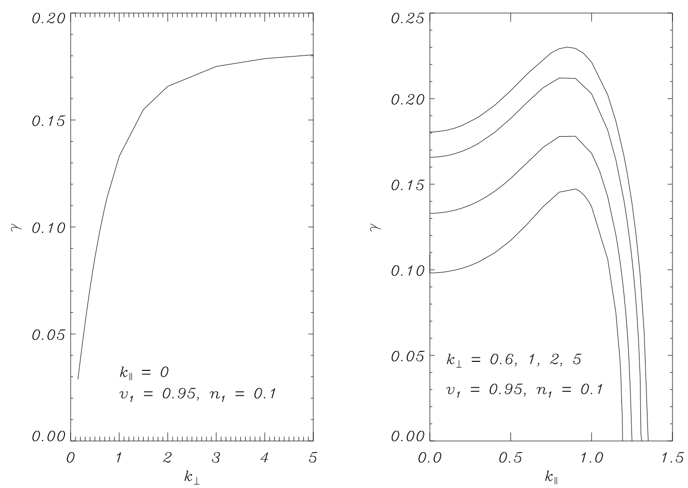

Interplay with “Weibel” instabilities?

Linear stability analysis and 3D fluid simulation (F. Califano) show that the relativistic “Weibel” instability of *counterstreaming, asymmetrical beams* (e.g. fast electrons current and slow return current) does *not* lead to filaments *unless* the initial beams have finite width (i.e. a given $k_\perp$).

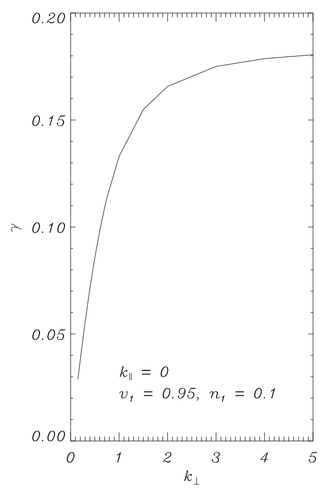

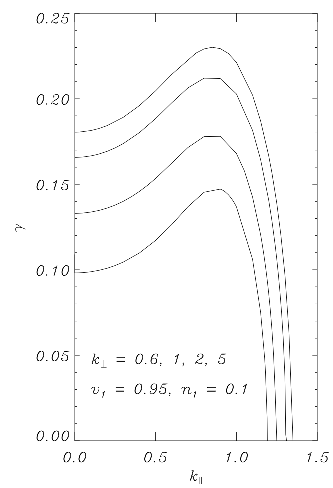

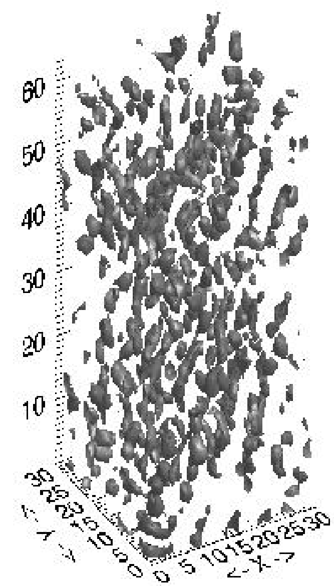

Interplay with "Weibel" instabilities?

Linear stability analysis and 3D fluid simulation (F. Califano) show that the relativistic "Weibel" instability of *counterstreaming*, *asymmetrical beams* (e.g. fast electrons current and slow return current) does *not* lead to filaments *unless* the initial beams have finite width (i.e. a given $k_\perp$).

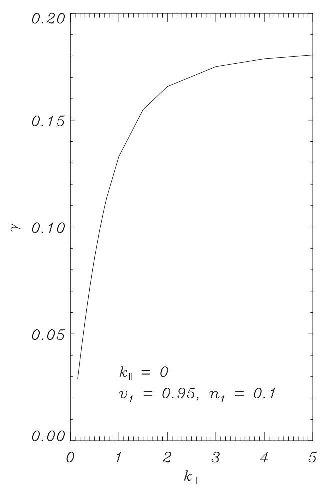

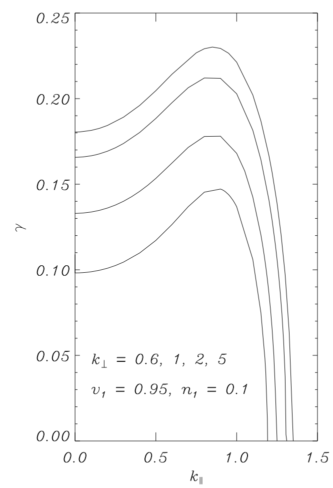

TSWD may "seed" Weibel filamentation by modulating the currents and/or the EM fields.

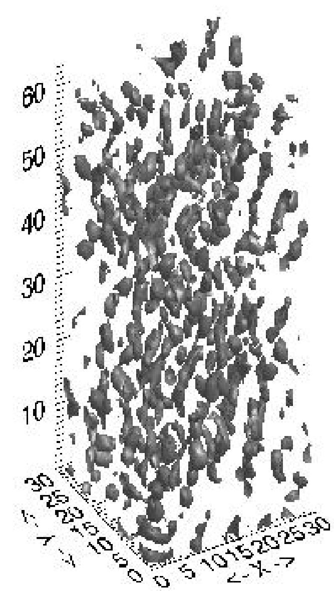

Interplay with “Weibel” instabilities?

Linear stability analysis and 3D fluid simulation (F. Califano) show that the relativistic “Weibel” instability of *counterstreaming, asymmetrical beams* (e.g. fast electrons current and slow return current) does *not* lead to filaments *unless* the initial beams have finite width (i.e. a given $k_\perp$).

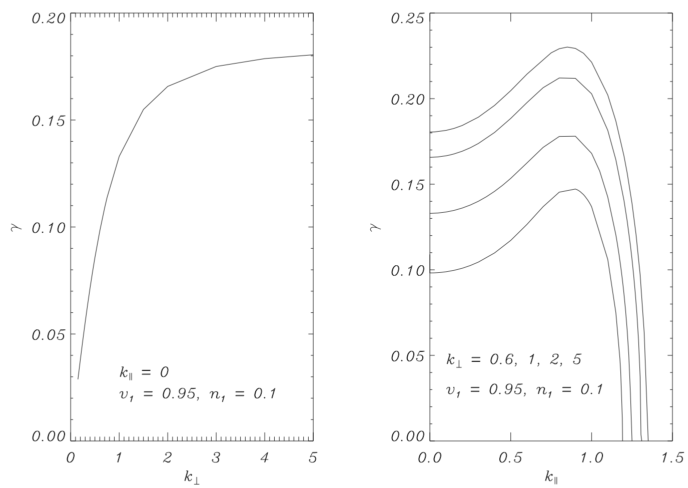

TSWD may “seed” Weibel filamentation by modulating the currents and/or the EM fields.

A. Macchi et al, Nucl. Fusion **43**, 362 (2003)

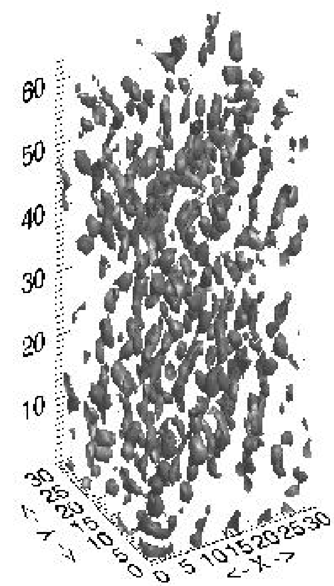

Future directions

- Theory: go beyond the quasi–linear (low amplitude) approximation

Future directions

- Theory: go beyond the quasi–linear (low amplitude) approximation
- Simulation:
  - characterise TSWD in a wider regime

Future directions

- Theory: go beyond the quasi–linear (low amplitude) approximation
- Simulation:
  - characterise TSWD in a wider regime
    (other parameters, oblique incidence,. . .)

Future directions

- Theory: go beyond the quasi–linear (low amplitude) approximation
- Simulation:
  - characterise TSWD in a wider regime
    (other parameters, oblique incidence,. . .)
  - investigate connection between TSWD and filamentation instabilities

Future directions

- Theory: go beyond the quasi–linear (low amplitude) approximation
- Simulation:
  - characterise TSWD in a wider regime
    (other parameters, oblique incidence,. . .)
  - investigate connection between TSWD and filamentation instabilities
    (interplay with Weibel–like instabilities?)

Acknowledgment

This was a Microsoft-free presentation.

Acknowledgment

This was a Microsoft-free presentation.

It has been prepared from a LaTeXsource on a Linux PC using the PPower4 package.

Acknowledgment

This was a Microsoft-free presentation.

It has been prepared from a LaTeX source on a Linux PC using the PPower4 package.

100% open source software!

Rough explanation for enhanced acceleration

- The modulation in p_x produced by SW is $\approx 30\%$

Rough explanation for enhanced acceleration

- The modulation in p_x produced by SW is $\approx 30\%$ although $a_{SW}^{(\omega)}/a^{(2\omega)} \approx 0.1$.

Rough explanation for enhanced acceleration

- The modulation in p_x produced by SW is $\approx 30\%$ although $a_{SW}^{(\omega)}/a^{(2\omega)} \approx 0.1$.

- Qualitative explanation based on the "non–adiabaticity parameter" $\eta = L/v_0 T$

  L: evanescence length, v_0: electron velocity, T: oscillation period

Rough explanation for enhanced acceleration

- The modulation in p_x produced by SW is $\approx 30\%$ although $a^{(\omega)}_{SW}/a^{(2\omega)} \approx 0.1$.

- Qualitative explanation based on the "non–adiabaticity parameter" $\eta = L/v_0 T$
  L: evanescence length, v_0: electron velocity, T: oscillation period
  Meaning: $\eta =$(transit time)/(oscillation period) ratio
  (small η means stronger non–adiabaticity)

- $\eta_{ESW}/\eta_{2\omega} = \sqrt{(\alpha-2)/(\alpha-1)} < 1$

$\longrightarrow$ enhanced contribution of SW in accelerating/decelerating electrons.